ANKARA YILDIRIM BEYAZIT UNIVERSITY

GRADUATE SCHOOL OF NATURAL AND APPLIED SCIENCES



OPTIMIZING THICKNESS DESIGN FOR BONDED FIBER-REINFORCED CONCRETE OVERLAYS ON ASPHALT PAVEMENTS: ADAPTING TO VARIED TRAFFIC, SUBGRADE, AND CLIMATE CONDITIONS IN TÜRKIYE

M.Sc. Thesis by

Duygu KAPLANCA

Department of Civil Engineering

July, 2025

ANKARA

OPTIMIZING THICKNESS DESIGN FOR BONDED FIBER-REINFORCED CONCRETE OVERLAYS ON ASPHALT PAVEMENTS: ADAPTING TO VARIED TRAFFIC, SUBGRADE, AND CLIMATE CONDITIONS IN TÜRKIYE

A Thesis Submitted to

The Graduate School of Natural and Applied Sciences of

Ankara Yıldırım Beyazit University

In Partial Fulfillment of the Requirements for the Degree of Master of Science of Civil Engineering, Department of Civil Engineering

by

Duygu KAPLANCA

July, 2025

ANKARA

M.Sc. THESIS EXAMINATION RESULT FORM

We have read the thesis entitled **"OPTIMIZING THICKNESS DESIGN FOR BONDED FIBER-REINFORCED CONCRETE OVERLAYS ON ASPHALT PAVEMENTS: ADAPTING TO VARIED TRAFFIC, SUBGRADE, AND CLIMATE CONDITIONS IN TÜRKIYE"** completed by **DUYGU KAPLANCA** under supervision of **ASSIST. PROF. DR. EMİN ŞENGÜN** and we certify that in our opinion it is fully adequate, in scope and in quality, as a thesis for the degree of Master of Science.

Assist. Prof. Dr. Emin ŞENGÜN

Supervisor

Prof. Dr. İ. Özgür YAMAN

Jury Member

Assist. Prof. Dr. Duygu DEMİRTÜRK

Jury Member

Prof. Dr. İlyas ÇANKAYA

Director

Graduate School of Natural and Applied Sciences

ETHICAL DECLARATION

I hereby declare that, in this thesis which has been prepared in accordance with the Thesis Writing Manual of Graduate School of Natural and Applied Sciences,

- All data, information and documents are obtained in the framework of academic and ethical rules,
- All information, documents and assessments are presented in accordance with scientific ethics and morals,
- All the materials that have been utilized are fully cited and referenced,
- No change has been made on the utilized materials,
- All the works presented are original,

and in any contrary case of above statements, I accept to renounce all my legal rights.

Date: …../07/2025 **Signature:**

Name & Surname: Duygu KAPLANCA

ACKNOWLEDGEMENTS

First of all, I would like to express my deepest gratitude to my supervisor Assist. Prof. Dr. Emin ŞENGÜN for all of his help, advice, encouragement, optimism, and friendly attitude during my research.

Beside my advisor, I deeply express my gratitude to Prof. Dr. Murat GÜLER for all of his help, confidence, and advice with my thesis.

I also appreciate my thesis examining committee members for their valuable contributions during my research period.

Among the numerous people who helped and encouraged me with this research, I would especially like to express my sincere gratitude to my entire family — including my mother, my father, my dear husband Yunus, and my lovely children Yağız Alp and Defne, for their invaluable support, understanding, and tolerance.

July, …… 2025 **Duygu KAPLANCA**

OPTIMIZING THICKNESS DESIGN FOR BONDED FIBER-REINFORCED CONCRETE OVERLAYS ON ASPHALT PAVEMENTS: ADAPTING TO VARIED TRAFFIC, SUBGRADE, AND CLIMATE CONDITIONS IN TÜRKIYE

ABSTRACT

Türkiye's Ministry of Transport and Infrastructure reports a growing demand for durable, long-life pavement systems due to the increasing number of freight and passenger traffic on highways. The existing road network is predominantly asphalt and chip-seal pavements, which require frequent maintenance and overlay applications under heavy traffic conditions. This study focuses on the alternative approach of Bonded Concrete Overlays on Asphalt (BCOA), which has gained attention in developed countries as a structurally efficient and durable solution.

The study presents a parametric design framework for BCOA using Pittsburgh University's BCOA-ME software, applied across ten pilot cities in Türkiye's diverse climatic regions: Afyonkarahisar, Erzurum, Eskişehir, İstanbul, İzmir, Kayseri, Konya, Mersin, Rize, and Şanlıurfa. The design scenarios included traffic volume categories, subgrade stiffness levels, HMA condition states, and joint spacing configurations. Fiber reinforcement effects were analyzed at different dosage levels, with 1,440 simulations conducted.

Synthetic fibers can reduce overlay thickness by improving fatigue resistance and post-cracking behavior. The average thickness reductions are around 24% for a fiber dosage of 3.5 kg/m³ and 19% for 2.5 kg/m³. Fiber reinforcement also optimizes joint spacing, allowing for longer slab dimensions without compromising structural performance. However, further experimental validation is needed to understand its influence on load transfer efficiency and crack control. Climatic factors, such as high solar exposure and high annual sunshine percentages, also affect overlay thickness demands. A user-accessible design tool is introduced as a first step towards developing a fully localized Mechanistic-Empirical (M-E) BCOA pavement design framework for Türkiye. The framework aims to evolve into a nationally calibrated design system incorporating local materials, climate data, and long-term field performance observations.

Keywords: Bonded Concrete Overlays on Asphalt, Pavement Design, Mechanistic-Empirical Approach, Sensitivity Analysis, Thickness Design Chart.

ASFALT KAPLAMALAR ÜZERİ BAĞLI LİF DONATILI BETON TAKVİYE TABAKALARININ KALINLIK TASARIMI: TÜRKİYE'DEKİ FARKLI TRAFİK, ZEMİN VE İKLİM KOŞULLARINA GÖRE OPTİMİZASYONU

ÖZ

Türkiye Ulaştırma ve Altyapı Bakanlığı, otoyollarda artan yük ve yolcu trafiği nedeniyle dayanıklı, uzun ömürlü kaplama sistemlerine yönelik talebin arttığını bildirmektedir. Mevcut yol ağı ağırlıklı olarak asfalt ve sathi kaplamalardan oluşmakta olup yoğun trafik koşullarında sık sık bakım ve onarım gerektirmektedir. Bu çalışmada gelişmiş ülkelerde tercih edilmeye başlanan asfalt üzeri bağlı beton takviye tabakası (BCOA) uygulama alternatifi üzerine yoğunlaşılmıştır.

Bu çalışma, Pittsburgh Üniversitesi'nin BCOA-ME yazılımını kullanarak, Türkiye'nin farklı iklim bölgelerindeki on pilot şehirde (Afyonkarahisar, Erzurum, Eskişehir, İstanbul, İzmir, Kayseri, Konya, Mersin, Rize ve Şanlıurfa) uygulanan BCOA için bir tasarım aracı sunmaktadır. Tasarım senaryoları trafik hacmi kategorilerini, temel zemin sertliği seviyelerini, mevcut asfalt durumlarını ve derz aralığı konfigürasyonlarını içermekte olup farklı miktarlarda fiber takviyesi etkileri analiz edilerek 1.440 simülasyon gerçekleştirilmiştir.

Sentetik fiberler, yorulma direncini ve çatlak sonrası davranışı iyileştirerek kaplama kalınlığını azaltmanın yanı sıra, yapısal performanstan ödün vermeden daha uzun döşeme boyutlarına izin vererek derz aralığını optimize etme potansiyeli de göstermiştir. Ortalama kalınlık azalmaları, 3.5 kg/m³ lif dozajı için yaklaşık %24 ve 2.5 kg/m³ için %19 civarında gözlemlenmiştir. Ancak, yük aktarım verimliliği ve çatlak kontrolü üzerindeki etkisini anlamak için daha fazla deneysel doğrulama gerekmektedir. Yüksek güneş ışığına maruz kalan ve yıllık güneş ışığı yüzdesi yüksek olan bölgelerde kaplama kalınlığı ihtiyacı artmıştır. Bu çalışmada Türkiye için kullanıcı erişimine açık bir kaplama tasarım aracı tanıtılmaktadır. Bu araç, yerel malzemeleri, iklim verilerini ve uzun vadeli saha performansı gözlemlerini içeren ulusal olarak kalibre edilmiş bir tasarım sistemine dönüşmeyi hedeflemektedir.

Anahtar kelimeler: Asfalt Üzeri Bağlı Takviye Beton Tabakası, Üstyapı Tasarımı, Mekanistik-Empirik Yaklaşım, Duyarlılık Analizi, Kalınlık Tasarım Tablosu.

CONTENTS

M.Sc. THESIS EXAMINATION RESULT FORM ii
ETHICAL DECLARATION iii
ACKNOWLEDGEMENTS iv
ABSTRACT v
ÖZ vi
NOMENCLATURE ix
LIST OF TABLES x
LIST OF FIGURES xi

CHAPTER 1 - INTRODUCTION 1
1.1 Background 1
1.2 Objective and Scope 2
1.3 Research Outline 3

CHAPTER 2 - LITERATURE REVIEW 4
2.1 Pavement and Traffic Context in Türkiye 4
2.2 Overview of BCOA Technology 10

CHAPTER 3 - METHODOLOGY 19
3.1 Design Requirements 19
3.2 Selection of Study Locations 20
3.3 Traffic Volume Calculation 21
3.4 Climate 25
3.4.1 EELTG (ΔT) for Fatigue Cracking 27
3.4.2 EELTG (ΔT) for Faulting 28
3.4.3 Determination EELTG' Inputs 29
3.5 Existing Structure HMA 30
3.6 PCC Overlay Strength Properties 35
3.7 Fiber Effect 36
3.7.1 Design Stress for Slabs Joint Spacing ≤ 4.5 ft (Small Slab) 39
3.7.2 No Fiber Condition 44
3.7.3 Fiber Volume 2.5 kg/m³ (4.0 lb/$yd3$) 44

3.7.4 Fiber Volume 3.5 kg/m³ (6.0 lb/$yd3$) 45
3.8 Reflective Cracking Potential 46
3.9 Faulting Analysis 47
3.10 Wheel Wander 48

CHAPTER 4 - RESULTS AND ANALYSIS 50
4.1 Fiber Effect 62
4.2 Climate Effect 65
4.3 Traffic Volume Effect 67
4.4 Joint Spacing Effect 68
4.4.1 Subgrade Effect 69
4.5 Structural Condition of the Asphalt layer 71

CHAPTER 5 - TOOL DEVELOPMENT 73

CHAPTER 6 - CONCLUSION AND RECOMMENDATIONS 74
6.1 Conclusion 74
6.2 Recommendations and Future Works 76

REFERENCES 77
CURRICULUM VITAE 83

NOMENCLATURE

AADT	Average Annual Daily Truck Traffic
ADT	Average Daily Traffic
AMDAT	Annual Mean Daily Average Temperature
BCOA	Bonded Concrete Overlay of Asphalt
BCOA-ME	Bonded Concrete Overlay of Asphalt Pavements Mechanistic-Empirical Design Guide
EELTG	Effective Equivalent Linear Temperature Gradient
EICM	The Enhanced Integrated Climatic Model
ESAL	Equivalent Single Axle Load
EU	European Union
FRC	Fiber Reinforced Concrete
GDH	Türkiye's General Directorate of Highways
HMA	Hot-Mix Asphalt
IMM	Istanbul Metropolitan Municipality
JPCP	Jointed Plain Concrete Pavements
M-E	Mechanistic-Empirical
MOR	Modulus of Rupture
PCC	Portland Cement Concrete
TÜİK	Turkish Statistical Institute
UHPFRC	Ultra-High-Performance Fiber-Reinforced Concrete
UTW	Ultra-Thin Whitetopping

LIST OF TABLES

Table 2.1 As of 2024 Road Network 4
Table 2.2 Summary information table for trial concrete roads 9
Table 3.1 Design variable values entered into the BCOA-ME Design Program. 20
Table 3.2 LDF factor 22
Table 3.3 Axles per 1000 trucks for various types of roads. Taken from "Design of Concrete Pavement for City Streets (2002)". 22
Table 3.4 Similar climate stations belong to provincial regions 27
Table 3.5 Freezing ratio regression coefficients 29
Table 3.6 Influence of Existing HMA Pavement Condition on Modulus Reduction and Damage Factor 30
Table 3.7 Composite Modulus of Subgrade Reaction, k-value 31
Table 3.8 Average values of HMA in Türkiye 35
Table 3.9 Experimentally determined limit values of stress factors for different types of fibers. 43
Table 4.1 Recommended C30 Concrete Overlay Thickness for Afyonkarahisar 52
Table 4.2 Recommended C30 Concrete Overlay Thickness for Erzurum 53
Table 4.3 Recommended C30 Concrete Overlay Thickness for Eskişehir 54
Table 4.4 Recommended C30 Concrete Overlay Thickness for İstanbul 55
Table 4.5 Recommended C30 Concrete Overlay Thickness for İzmir 56
Table 4.6 Recommended C30 Concrete Overlay Thickness for Kayseri 57
Table 4.7 Recommended C30 Concrete Overlay Thickness for Konya 58
Table 4.8 Recommended C30 Concrete Overlay Thickness for Mersin 59
Table 4.9 Recommended C30 Concrete Overlay Thickness for Rize 60
Table 4.10 Recommended C30 Concrete Overlay Thickness for Şanlıurfa 61

LIST OF FIGURES

Figure 2.1 Domestic Passenger and Freight Transportation Rates by Transportation Types in 2022 5

Figure 2.2 Tonne-km, Passenger-km and vehicle-km values by years 5

Figure 2.3 Asphalt construction, repair and renewal by years (31.12.2023) 6

Figure 2.4 Number of cars per 1000 people in European Countries (2022) 7

Figure 2.5 Percentages of increase in travel and transportation on highways, state and provincial roads by years compared to 2005 8

Figure 2.6 IMM (Istanbul Metropolitan Municipality) Metrobus Line. 8

Figure 2.7 Flexible and rigid pavement load distribution 10

Figure 2.8 System of concrete overlays and bonded concrete overlay section 11

Figure 2.9 Stress distribution on overlay mechanism due to traffic loads (a) bonded overlays, (b) unbonded overlays 12

Figure 2.10 Suitable HMA pavement conditions for a BCOA and characteristics of a good and poor BCOA candidates 13

Figure 2.11 Good and Fair conditions of existing asphalt 13

Figure 2.12 Reflecting cracking mechanism and real-world example in thin bonded whitetopping 14

Figure 2.13 Interface debonding in BCOAs 16

Figure 2.14 Advantages of Incorporating Macrofibers in Concrete Overlays [26] .. 16

Figure 2.15 Short fibers enhance tensile strength by bridging microcracks; long fibers improve ductility by bridging macrocracks 17

Figure 3.1 Köppen-Geiger climate type map of the Türkiye and selected provinces 21

Figure 3.2 Map of AMDAT Region..... 25

Figure 3.3 Annual concentrating solar resource map of USA 26

Figure 3.4 Transverse cracking in an existing HMA pavement 31

Figure 3.5 Fatigue Severity Levels 32

Figure 3.6 Typical Distresses Observed in Hot Mix Asphalt (HMA) Pavements ... 32

Figure 3.7 Flowchart for Evaluating the Suitability of BCOA as a Rehabilitation Option 34

Figure 3.8 A comparison of normal, FRC (fiber reinforced) and ultra high performance FRC types of concrete in tensile stress and strain..... 36

Figure 3.9 ASTM C1609 typical load-deflection graphs and necessary parameters for calculating 38

Figure 4.1 PCC Thickness vs Fiber Amount Graphics of ten provinces in case of fiber

quantity increasing from zero to 3.5 kg/m3 (for the case of ESAL low-moderate, fatigue-Adequate, subgrade k value-moderate, joint spacing 1x1 m)..... 64

Figure 4.2 PCC Thickness vs Fiber Amount Graphic of ten provinces (for the case of ESAL low-moderate, fatigue-Adequate, subgrade k value-moderate, joint spacing 1x1 m). 64

Figure 4.3 PCC Thickness vs Fiber Amount Graphic of ten provinces (for the case of ESAL-high, fatigue-Adequate, subgrade k value-poor, joint spacing 2x2 m)..... 65

Figure 4.4 PCC Thickness vs Fiber Amount Graphic of ten provinces (for the case of ESAL-low, fatigue-Adequate, subgrade k value-poor, joint spacing 2x2 m)..... 66

Figure 4.5 PCC Thickness vs Fiber Amount Graphic of ten provinces (for the case of ESAL low-moderate, fatigue-Adequate, subgrade k value-moderate, joint spacing 1x1 m). 67

Figure 4.6 PCC Thickness vs Traffic Volume Graphics of ten provinces (for the case of fatigue-Adequate, subgrade k value-moderate, fiber content-max and joint spacing is 1x1 m)..... 68

Figure 4.7 PCC Thickness vs Fiber Content-Cities Graphic of ten provinces in case of small and large slab (for the case of ESAL low-moderate, fatigue-Adequate, subgrade k value-moderate). 69

Figure 4.8 PCC Thickness vs Subgrade Graphic of ten provinces (for the case of ESAL low-moderate, fatigue-Adequate, joint spacing 1x1 m and no fiber) 70

Figure 4.9 PCC Thickness vs Subgrade Graphic of ten provinces (for the case of ESAL low-moderate, fatigue-Adequate, joint spacing 2x2 m and no fiber) 70

Figure 4.10 PCC Thickness vs Joint Spacing Graphics of ten provinces (k value from poor to good while thickness variation for small and large slab of ten provinces for the case of traffic-low moderate, fatigue-Adequate, k value-poor to good, no fiber)..... 71

Figure 4.11 PCC Thickness vs Fatigue Graphics of ten provinces (for the case of ESAL low-moderate, fatigue-Adequate, k value-moderate, joint spacing 1x1 m and Fiber Content 3.5 kg/m3)..... 72

CHAPTER 1

INTRODUCTION

1.1 Background

Data from Türkiye's Ministry of Transport and Infrastructure indicate that highways account for approximately 89% of freight and 91% of passenger transportation. Over the last decade, freight and passenger traffic have increased by 44% and 30%, respectively, highlighting growing pressure on the road network. Although highways and state roads comprise only about half of Türkiye's total road system, they bear a disproportionately high volume of transport demand, necessitating extensive maintenance and rehabilitation efforts.

In contrast to practices in developed countries—where concrete pavements are preferred for high-traffic routes due to their durability—Türkiye's Road network is still dominated by flexible pavements such as asphalt and chip seals. Although technical specifications for rigid pavements were introduced in 2016, concrete road implementation remains limited. Nevertheless, awareness of more durable alternatives is gradually increasing, with bonded concrete overlays on asphalt (BCOA) emerging as a promising solution for long-term pavement performance.

The global application of Portland cement concrete (PCC) overlays as a rehabilitation technique for both PCC and hot-mix asphalt (HMA) pavements has steadily increased over recent decades. These overlays offer several benefits, including reduced life-cycle costs, improved structural capacity, lower maintenance demands, and extended service life. The use of PCC overlays dates back to 1913 for PCC pavements and 1918 for HMA pavements. Since the mid-1960s, highway agencies have increasingly investigated alternative pavement rehabilitation strategies. Among these, "whitetopping (BCOA)" the resurfacing of HMA pavements with PCC—has attracted growing research interest within the broader context of PCC overlay technologies [1].

Concurrently, a major development in pavement engineering has been the transition from empirical pavement design methods to mechanistic-empirical (ME) approaches. Traditional empirical methods, while grounded in observed performance data, often fall short in forecasting pavement behavior under varying traffic loads and environmental conditions. ME design frameworks, in contrast, integrate fundamental engineering principles with empirical calibration, enabling more accurate and reliable pavement performance predictions. Within this framework, the mechanistic-empirical design of bonded concrete overlays on asphalt pavements (BCOA-ME) has gained increasing attention in both academic studies and field practice—particularly in efforts to optimize overlay thickness for durability and cost-effectiveness [2,3].

This thesis aims to analyze and develop recommended overlay thickness design charts adapted to the conditions of various Turkish cities representing different climate zones. The findings propose practical design recommendations based on key factors such as subgrade quality, traffic loading, and climatic conditions. Additionally, the study investigates variations in design performance under different fiber reinforcement scenarios and evaluates their effectiveness across a range of joint spacing configurations.

1.2 Objective and Scope

This study conducted a total of 1,440 bonded concrete overlay (BCOA) design simulations—both fibrous and non-fibrous—for ten provinces across Türkiye, each representing distinct climatic conditions. The primary objective is to develop practical design charts and to analyze the key factors influencing BCOA thickness design, including traffic loading, subgrade conditions, climate variations, fiber reinforcement, and joint spacing configurations. By doing so, the study aims to assist pavement engineers and designers in evaluating overlay design parameters more comprehensively for asphalt pavements requiring structural rehabilitation.

All calculations and outputs are presented in detail in the methodology section. The BCOA-ME software, a finite element-based design tool developed by the University of Pittsburgh, was utilized throughout the study. This software enables efficient and

accurate thickness estimation for bonded concrete overlays using a mechanistic-empirical design approach, allowing for the rapid evaluation of multiple scenarios.

Furthermore, a user-friendly design interface has been developed, enabling users to independently select design variables such as traffic volume, subgrade type, existing asphalt condition, fiber content, and joint spacing. This tool, accessible via QR code and hyperlink for selected provinces in Türkiye, provides practical guidance for engineers conducting BCOA thickness design under varying field conditions.

 http://anabasist.xyz/

1.3 Research Outline

Chapter 2 presents a comprehensive literature review on bonded concrete overlays, including international practices, data from Türkiye's General Directorate of Highways (GDH), and an overview of pilot projects implemented across the country.

Chapter 3 details the design methodologies and calculation procedures employed in determining the required PCC overlay thickness, with a focus on the mechanistic-empirical (M-E) approach utilized by the BCOA-ME software.

Chapter 4 presents the results and findings of the study, providing detailed comparisons based on key design variables such as traffic loading, subgrade conditions, climate, fiber reinforcement, and joint spacing. The chapter concludes with a brief discussion and summary of the key insights drawn from the analysis.

Chapter 5 introduces a user-friendly design tool developed as part of this study. This tool integrates the results obtained from the BCOA-ME software and enables practitioners to perform scenario-based thickness design for selected provinces in Türkiye.

Chapter 6 concludes with a summary of the thesis that focuses on the analysis's conclusions and offers recommendations for additional research.

CHAPTER 2

LITERATURE REVIEW

2.1 Pavement and Traffic Context in Türkiye

Understanding the current state of Türkiye's Road infrastructure is essential for evaluating the need for alternative pavement solutions. As of 2024, data from the General Directorate of Highways (GDH) reveals that approximately 44% of the nation's highways and state roads are surfaced with asphalt concrete (flexible pavement), while 52% are covered with chip-seal pavements, as shown in Table 2.1.

Table 2.1 Road Network Distribution in Türkiye as of 2024 [4].

ROAD NETWORK BY SURFACE TYPE-KM							
As of 01.01.2024							
	Asphalt Concrete	**Chip-Seal**	**Concrete Block**	**Stabilized**	**Soil**	**Other Roads**	**Total**
Highway (*)	3726	-	-	-	-	-	3726
State Roads	20135	10387	45	22	-	275	30864
Provincial Roads	6018	25182	225	276	299	2064	34064
TOTAL	29879	35569	270	298	299	2339	68654

DIVIDED ROADS (KM)	
01.01.2024	
Highways	3726
State Road	21680
Provincial Road	2294
Total	27700

(*) The highway length includes the highways constructed and put into service with Build-Operate-Transfer.

As seen in Figure 2.1, data from the Ministry of Transport and Infrastructure further indicate that highways play a dominant role in freight and passenger transportation in Türkiye, accounting for 89.3% and 91.2%, respectively, compared to maritime, air, and rail mode [5]. Although highways and state roads represent approximately half of Türkiye's total road network, they carry a disproportionately high share of national transport demand. This heavy reliance on the road network, combined with a 44% increase in freight traffic and a 30% increase in passenger traffic over the past decade, has created an urgent need for continuous maintenance and major pavement rehabilitation [6].

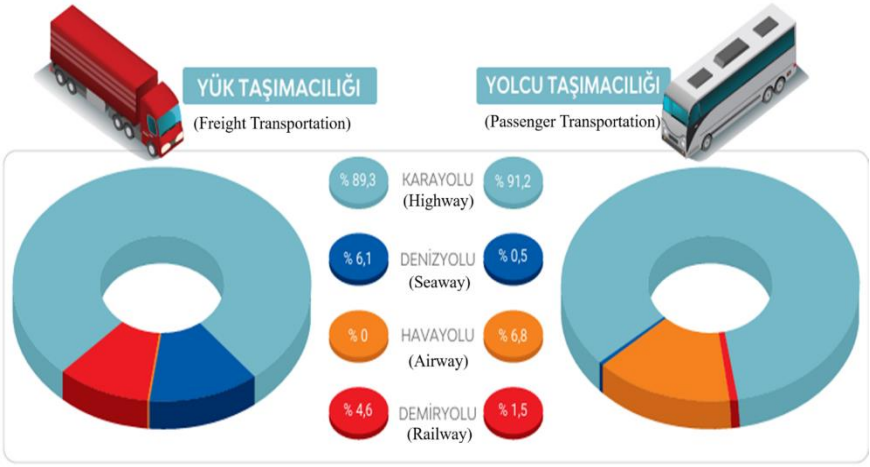

Figure 2.1 Domestic Passenger and Freight Transportation Rates by Transportation Types in 2022 [5]

As seen in Figure 2.2, road freight transport in Türkiye reached 335.126 billion ton-km, while passenger transport totaled 380.178 billion passenger-km, with overall road usage amounting to 154.502 billion vehicle-km in 2023 [6].

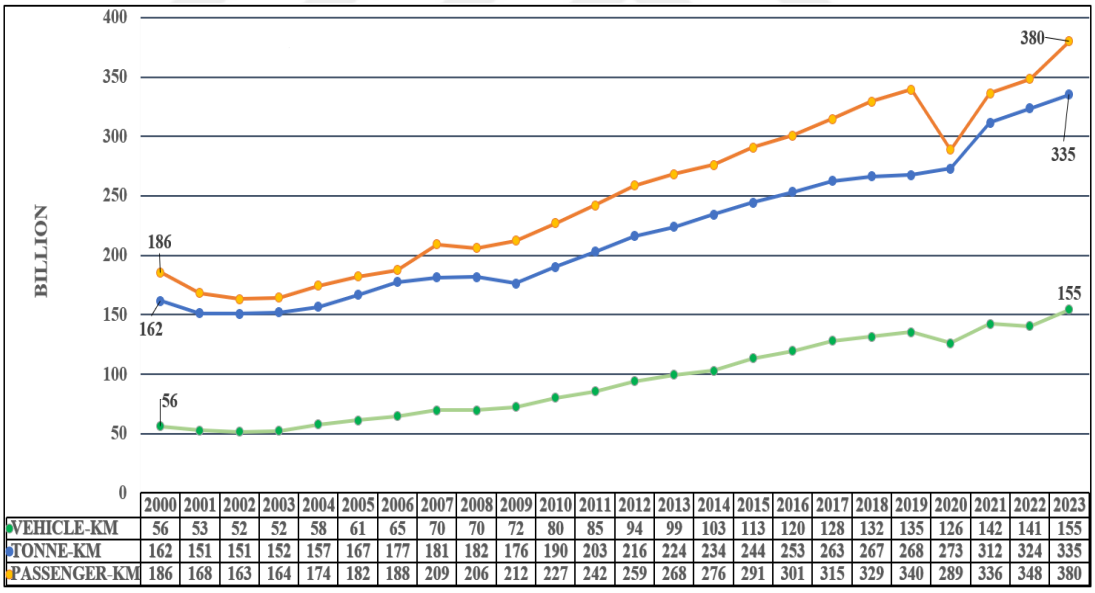

	2000	2001	2002	2003	2004	2005	2006	2007	2008	2009	2010	2011	2012	2013	2014	2015	2016	2017	2018	2019	2020	2021	2022	2023
VEHICLE-KM	56	53	52	52	58	61	65	70	70	72	80	85	94	99	103	113	120	128	132	135	126	142	141	155
TONNE-KM	162	151	151	152	157	167	177	181	182	176	190	203	216	224	234	244	253	263	267	268	273	312	324	335
PASSENGER-KM	186	168	163	164	174	182	188	209	206	212	227	242	259	268	276	291	301	315	329	340	289	336	348	380

Figure 2.2 Tonne-km, Passenger-km and vehicle-km values by years [6].

Between 2005 and 2022, the vehicle-km metric increased by 143.3%, ton-km by 106.3%, and passenger-km by 99.9%, highlighting significant growth in road transportation demand over the past two decades. As of 2023, approximately 13% of the nation's highways required major pavement rehabilitation, which entails

significant structural reconstruction. Maintenance demands have been met by substantial efforts, including 839 km of HMA pavement construction and rehabilitation and 6,374 km of chip-seal pavement work completed in 2023 alone, as seen in Figure 2.3 [4].

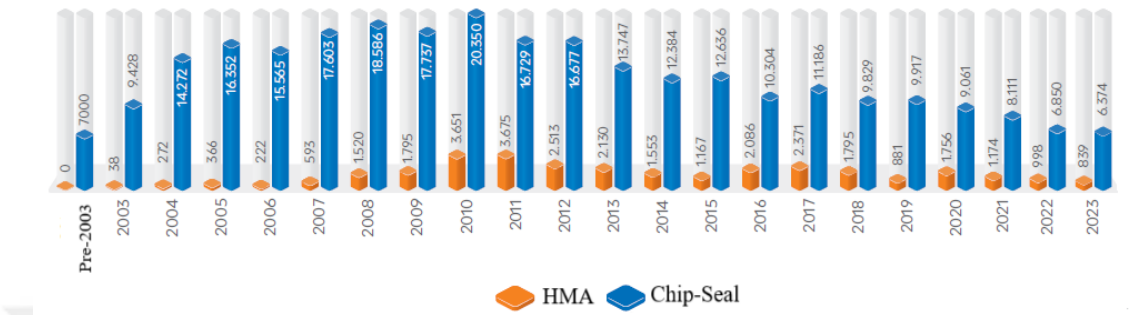

Figure 2.3 Asphalt construction, repair and renewal by years (31.12.2023) [5].

Cumulatively, between 2003 and 2023, these figures amounted to 31,395 km of HMA pavement and 273,698 km of chip-seal pavement. The allocated budget for highway and state road repairs in 2024 underscores this effort, with 4.7 billion TL designated for highways and 37.1 billion TL for state roads. Additionally, Türkiye's increasing vehicle ownership-currently standing at around 28.7 million registered vehicles, according to TÜİK December 2023 data—increases the demand for higher-standard roads. As seen in Figure 2.4, with vehicle ownership rates of 167 cars per 1,000 people (compared to an EU average of 531), Türkiye is projected to see continued growth in traffic density, placing further strain on the existing infrastructure. As traffic volume and heavy-load transport requirements rise, maintenance costs increase, showing the need to explore new, more resilient pavement technologies.

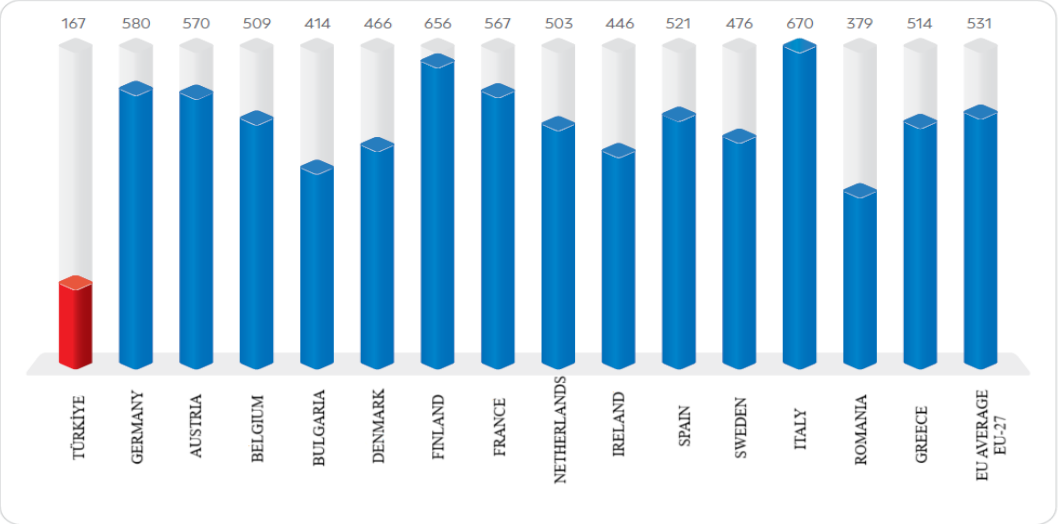

Figure 2.4 Number of cars per 1000 people in European Countries (2022) [5].

In many developed countries, concrete pavements are preferred for roads subjected to heavy traffic due to their durability and load-bearing capacity. For instance, in the United States, concrete pavements support a substantial share of traffic on high-volume highways. Similarly, in Canada's Quebec province, although concrete roads comprise only 4% of the network, they accommodate approximately 75% of total traffic. In Europe, concrete pavements are extensively utilized, particularly in Germany, Austria, and Belgium. In Germany, concrete accounts for about one-fourth of high-traffic highways; in Austria, three-fourths; and in Belgium, nearly half. Furthermore, in Belgium, concrete overlays are used for 60% of village roads, highlighting their versatility and long-term performance [7]. As seen in Figure 2.5, Between 2005 and 2022, the vehicle-km metric increased by 143.3%, ton-km by 106.3%, and passenger-km by 99.9%, highlighting significant growth in road transportation demand over the past two decades.

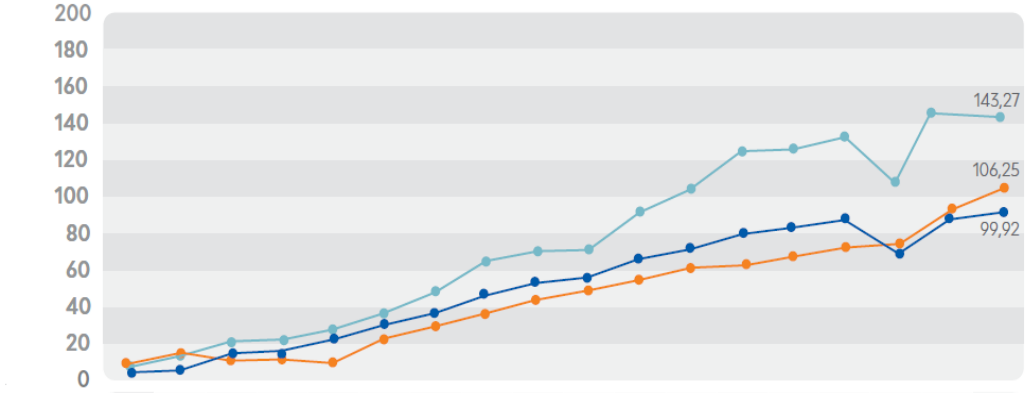

	2005	2006	2007	2008	2009	2010	2011	2012	2013	2014	2015	2016	2017	2018	2019	2020	2021	2022
Vehicle-Km	5,82	11,79	20,50	20,78	25,39	38,70	48,00	62,70	72,12	78,28	96,09	107,16	121,57	127,86	134,54	118,21	146,64	143,27
Tonne-Km	6,36	13,10	15,61	15,99	12,50	21,37	29,47	37,79	42,84	49,50	55,77	61,39	67,51	69,91	70,59	73,99	98,80	106,25
Passenger-Km	4,50	7,62	19,97	18,24	21,89	30,18	38,98	48,51	53,85	58,38	66,79	72,59	80,56	88,95	94,82	65,79	92,87	99,92

Figure 2.5 Percentages of increase in travel and transportation on highways, state and provincial roads by years compared to 2005 [5].

In Türkiye, concrete pavements are anticipated to play a crucial role in extending the service life of high-traffic, deformation-prone roads while reducing life cycle costs. Although GDH released technical specifications for concrete pavements in 2016, rigid pavement usage remains limited, with only 8.1 km of concrete roads under the GDH's purview, including pilot projects in Afyon-İşçehisar, Hasdal Kavşağı-Kemerburgaz, Ordu-Ulubey National Road, and Karamürsel City Crossing with detailed information is shown in Table 2.2. And also In Istanbul, a total of 42 kilometers of two-way roads have been covered with concrete which is called 'White Road', as seen in Figure 2.6 so that a total of 58 kilometers of metrobus roads on the European side have been permanently renovated with concrete material.



Figure 2.6 IMM (Istanbul Metropolitan Municipality) Metrobus Line [8].

Table 2.2 Summary information table for trial concrete roads [9]

Concrete Roads Data	Afyon-İçsehisar	Hasdal-Kemerburgaz	Ordu-Ulubey State Road	Karamürsel City Crossing
Road Type	JPCP	JPCP	JPCP	JPCP
Region	3rd	1st	7th	1st
Km	5+700-7+700	40+000-43+500	5+000-6+000	38+400 –40+000
Build Date	2004	2006	2007	2010
Project Duration	30 years	30 years	30 years	30 years
Protocol Between	KGM - TÇMB	KGM - TÇMB	KGM - BOREN	KGM
Length of concrete road	2 km	3.5 km	1 km	1.6 km
Platform Width	12 m	10,5 m	2x10,5 m	2 x 8.5 m
Number of Lane	3	2	2 x 2	2 x 2
Joint Spacings	5 m	5 m	4,5 m	4,5 m
Concrete thickness	27 cm	32 cm, 27 cm	28 cm	30 cm
Existing Structure	Chip-Seal	Primer on plent-mix 5 cm HMA	Chip-Seal	6 cm Binder
Cement Type	CEM I 42,5 and Silica Fume	CEM I 42,5	Boron Added	CEM I 42,5 R
Cement Amount	375 kg/m³	400 kg/m³	350 kg/m³	378 kg/m³
Water / Cement	0,41-0,45	≤ 0,35	~ 0,30	~ 0,43
Aggregate Properties	Crushed gravel, crushed sand, Dmaks 32 mm	Natural sand and crushed stone Dmaks 32 (mm)	Melet- Crushed stone Dmaks 25 mm	Crushed gravel, crushed sand, Dmaks 25 mm

In Türkiye, the growing traffic and freight demand has placed significant pressure on the existing road network, where approximately 65% of highways are surfaced with asphalt concrete and 33% with chip seal. Despite covering only half of the national network, highways carry over 89% of freight and 91% of passenger transport, leading to frequent maintenance needs, especially under heavy traffic. While technical specifications for rigid pavements were introduced in 2016, concrete pavement use remains limited. In contrast, many developed countries utilize concrete overlays, particularly BCOA, for their durability and cost-effectiveness. Given Türkiye's increasing vehicle ownership and the growing demands of pavement maintenance, BCOA presents an effective solution for extending pavement service life, improving structural performance, and minimizing long-term rehabilitation expenses. Additionally, BCOA is particularly beneficial for heavily trafficked areas prone to persistent rutting and other functional distresses commonly associated with asphalt pavements, such as friction loss and excessive noise.

2.2 Overview of BCOA Technology

Based on the characteristics of the materials utilized, highway pavements are classified into two primary categories: flexible and rigid. It is well recognized that numerous factors, including project design, application method, construction conditions, maintenance/repair conditions, climatic and environmental conditions, and comfort between rigid and flexible pavements. Concrete roads are a type of pavement made of cement concrete that transmits loads to the base. They consist of a granular subbase/base layer, weak concrete base layer, or concrete slab laid on a bituminous layer. Flexible pavements, on the other hand, can transmit and distribute traffic loads to the soil through the pavement. The structural capacity of rigid pavements depends on the concrete slab's load spreading capability and the thickness of each layer. The influence of soil strength on the thickness of rigid pavement is less than that of flexible pavements. The concrete slab's larger modulus of elasticity allows it to act as a beam resting on the elastic subgrade, transmitting traffic loads over a larger area than flexible pavements as seen in Figure 2.7 [9].

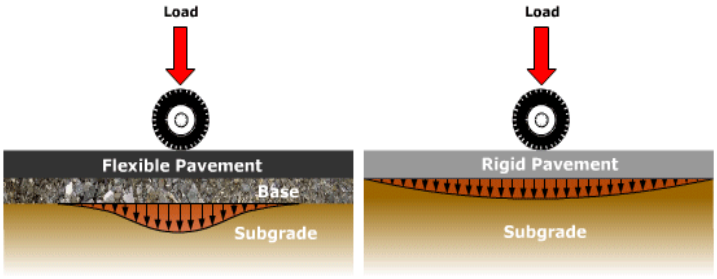

Figure 2.7 Flexible and rigid pavement load distribution [18]

In the early stages of concrete resurfacing, most applications involved simple, unreinforced concrete layers placed over unprepared surfaces in relatively thick sections. Over time, with accumulated field experience, these practices evolved into a broader family of resurfacing techniques suited to a variety of conditions, most notably, whitetopping or PCC overlays applied over asphalt pavements. The selection of an appropriate resurfacing technique typically depends on several key factors, including the condition of the existing pavement, cost-effectiveness, material

availability, traffic management requirements, constructability, and the engineer's professional judgment. Among these considerations, the interface condition between the overlay and the underlying pavement plays a critical role in determining the long-term performance of the resurfacing system.[11].

Interfaces fall into two general categories as shown in Figure 2.8: bonded and unbonded. Unbonded concrete layers show that specific precautions have been taken to ensure that there is no bond between them. Being bonded means that extra attention is made to enhance the layers' ability to bond, whereas being partially bound suggests that bonding is not significant [12].

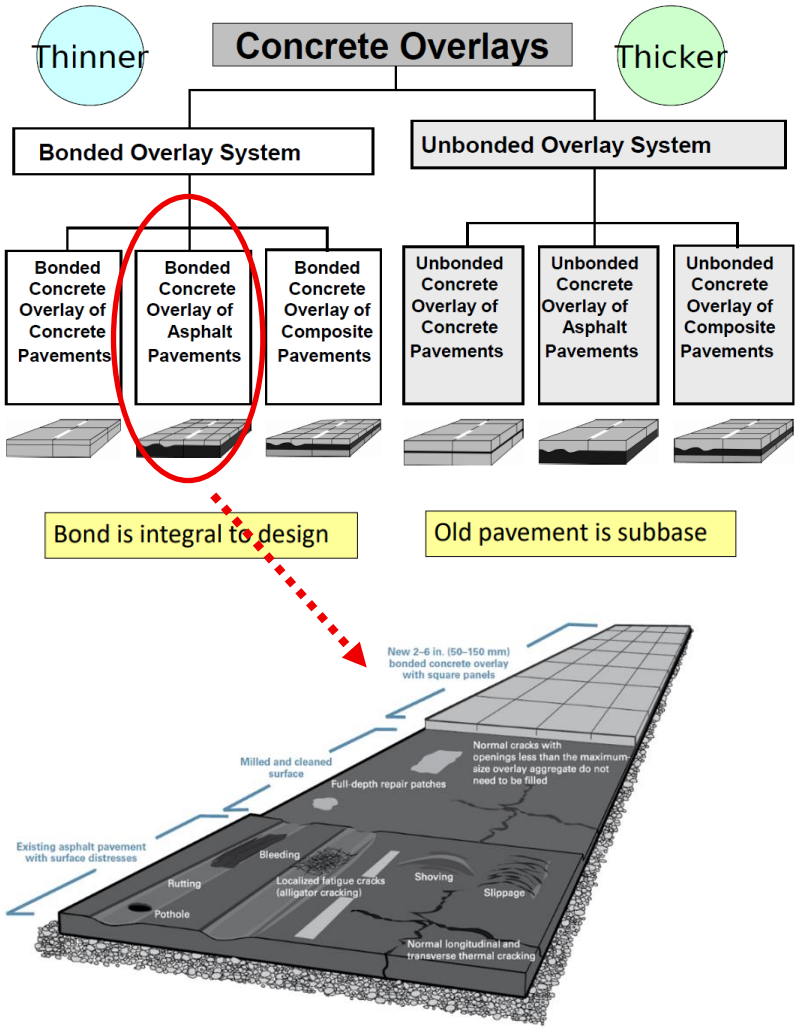

Figure 2.8 System of concrete overlays [12] and bonded concrete overlay section [13]

In pavement systems, the bonding condition between the overlay and the underlying layer significantly influences the stress distribution under loading. In bonded overlays, the concrete layer is fully adhered to the existing asphalt or concrete substrate, resulting in monolithic behavior, as shown in Figure 2.9-a. Under bending, the system acts as a single composite section, and a single neutral axis is formed across the combined depth. This allows compressive and tensile stresses to be distributed efficiently across both layers, enhancing structural performance. In contrast, unbonded overlays lack sufficient adhesion, leading the overlay and base layer to behave independently under load, as shown in Figure 2.9-b. As a result, each layer develops its own internal bending response with separate neutral axes, which can lead to inefficient load transfer and higher stress concentrations, particularly at the interface. This difference in structural response has critical implications for both performance and design, with bonded overlays offering durability and reduced risk of reflective cracking due to their integrated action.

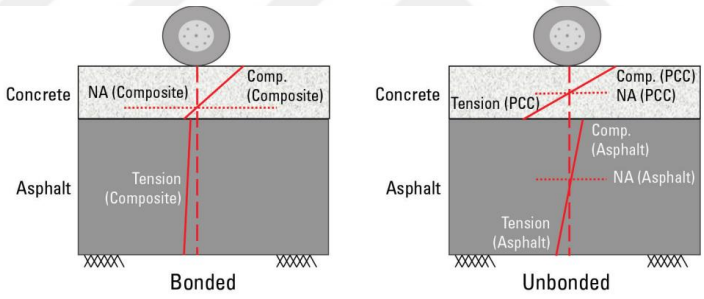

(a) (b)

Figure 2.9 Stress distribution on overlay mechanism due to traffic loads (a) bonded overlays, (b) unbonded overlays [14]

BCOAs are a category of resurfacing techniques in which a new concrete layer is placed over an existing pavement to improve structural performance and surface condition. While bonded overlays can be applied to both existing concrete and asphalt pavements, this study focuses on overlays bonded to asphalt (HMA) layers. In such applications, the existing asphalt surface must be in fair to good condition, as shown in Figure 2.10, but structurally insufficient to carry the projected [15].

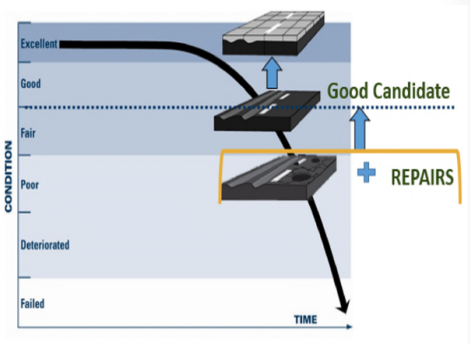

GOOD CANDIDATE	POOR CANDIDATE
Stable support conditions (Localized weak area can be strengthened)	Significant structural deterioration
Surface distresses	Stripping of lower HMA layers
Temperature cracking	Poor drainage
Minimum of 3 to 4 inches of HMA remaining after milling	Inadequate or uneven support conditions

Figure 2.10 Suitable HMA pavement conditions for a BCOA and characteristics of a good and poor BCOA candidates [15,16]

The purpose of the BCOA is to increase the structural capacity, eliminate surface defects such as rutting, shoving, minor alligator cracking, or thermal cracking and/or improve surface friction, noise, and rideability of the existing asphalt pavement (Figure 2.11). The BCOA, generally 5 to 15 cm thick, is designed to act in together with the underlying asphalt, forming a durable monolithic structure through a strong interface bond [17]. For the bond to be effective, proper surface preparation is essential to ensure cleanliness and adequate macrotexture. In some cases, pre-overlay repairs may be necessary to address severe distresses such as cracking, spalling, patching, punchouts, pumping, or settlement/heaving, in order to minimize the risk of reflective cracking.

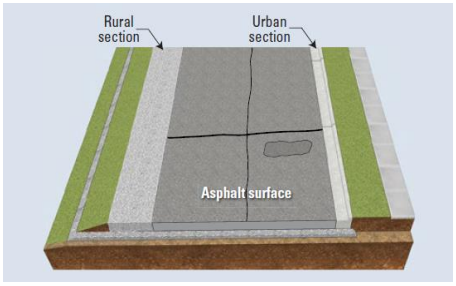

(a) Good- minor cracking

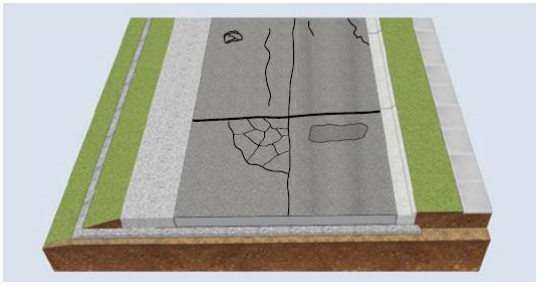

(b) Fair- potholes, block cracking, or thermal cracking

Figure 2.11 Good and Fair conditions of existing asphalt [14]

Reflection cracking in BCOA systems is influenced by stresses induced by both traffic loading and uniform temperature changes, as illustrated in Figure 2.12. In winter, thermal contraction of the HMA layer induces stress concentrations at the base of the concrete overlay, particularly near the tip of existing cracks in the underlying asphalt. These cracks can propagate upward through the concrete overlay when vehicle loads further increase the tensile stresses at the bottom of the overlay. The combined effects of load-related and temperature-induced stresses are supported by observations that reflection cracks appear more rapidly in driving lanes than in passing lanes and tend to form during winter and early spring conditions [18]. Since eliminating reflection cracking entirely is challenging, controlling its development is a common approach. This is typically achieved by sawing a joint in the overlay directly above each existing transverse joint shortly after placement. These joints are then sealed and maintained in the same manner as conventional pavement joints to accommodate movement and reduce stress concentrations [19].

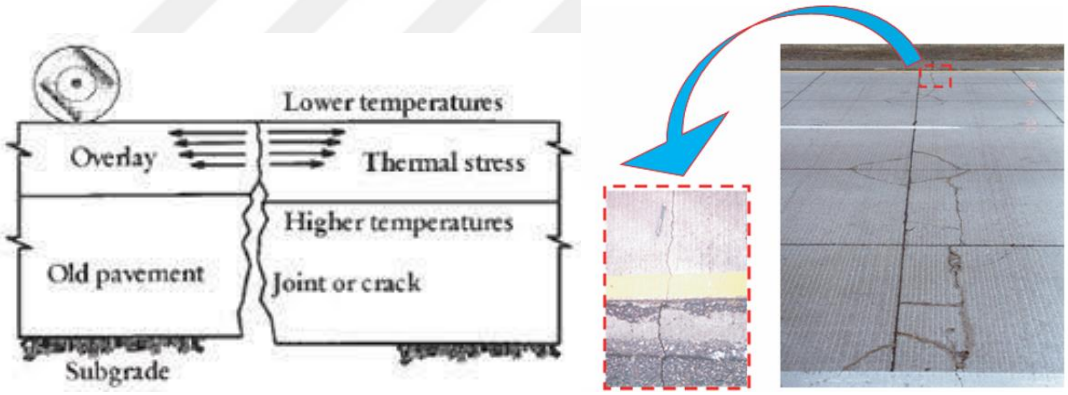

Figure 2.12 Reflecting cracking mechanism and real-world example in thin bonded whitetopping [18,20]

BCOA systems can extend the service life of pavements by approximately 20 years and represent a cost-effective rehabilitation option for moderately damaged asphalt surfaces. Their popularity comes from the relatively thin overlay thickness required and the ease of construction [21].

As performance data from completed projects become available, enhanced design guidelines can be developed, further promoting their adoption. Essential factors

influencing these designs include traffic loads, climate conditions, existing asphalt pavement structure, and concrete mixture properties. BCOA design considers economic and practical aspects alongside mechanical criteria. The thickness design is sensitive to several input parameters, notably traffic loads (commonly expressed as equivalent single axle loads—ESALs), temperature gradients, existing asphalt modulus, fiber reinforcement content, and joint spacing. Although various traffic analysis methods exist, the ESAL approach remains widely employed. Accurately estimating ESALs is crucial, as they significantly impact the performance of bonded overlays. The current pavement condition affects drainage efficiency, load transfer capability, and the modulus of rupture. To prevent overlay conservative thickness designs, pre-overlay repairs are typically performed to address significant drainage or load transfer issues before applying the bonded overlay [22]. To decide if a bonded overlay is appropriate for a project, a pavement evaluation is essential. The structural condition of the current pavement, predicted support values, milling needs, and the remaining three inches (7.62 cm) of asphalt are important findings [14].

To prevent excessive drying shrinkage in concrete overlays, careful attention must be given to concrete mixture design. Although proper curing practices can significantly reduce early-age shrinkage, the selected mixture proportions still greatly influence the overall shrinkage behavior of the overlay. Additionally, thorough surface preparation is critical. As illustrated in Figure 2.13, interface debonding represents one of the primary challenges in BCOA systems. Debonding at the concrete-asphalt interface often occurs due to excessive shrinkage in the concrete overlay and/or inadequate surface preparation [23,24]. When subjected to wheel loads, specific overlay areas may develop tensile stresses; combined with existing joints or cracks, these stresses can exacerbate debonding between the concrete overlay and the asphalt substrate, primarily due to their differential mechanical responses [25].

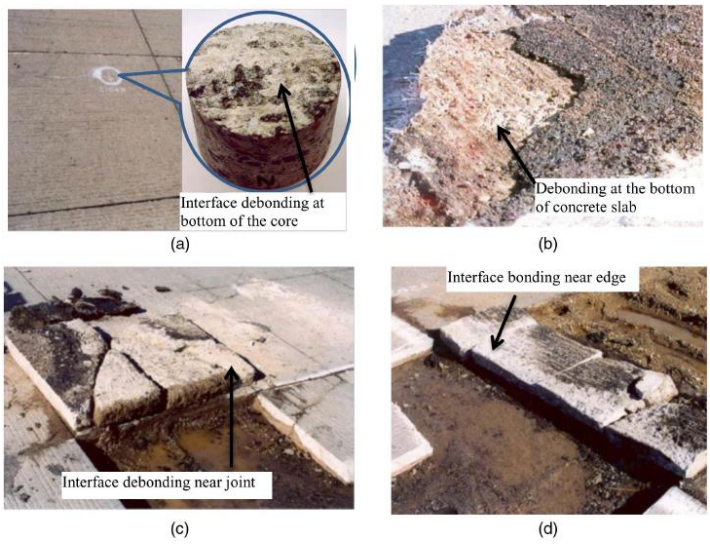

Figure 2.13 Interface debonding in BCOAs [23]

The flexural performance and load-bearing capacity of concrete can be significantly enhanced by the inclusion of macro fibers, especially after cracking has occurred in the slab. These fibers help control crack propagation along the substrate–overlay interface and contribute to the effectiveness of contraction joints and post-cracking behavior. As a result, fiber reinforcement enables the use of thinner overlays while extending service life and improving overall pavement fatigue performance, as summarized in Figure 2.14.

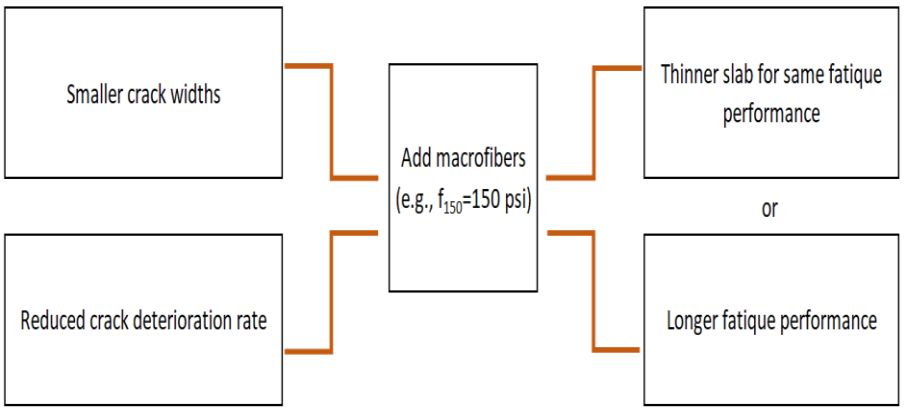

Figure 2.14 Advantages of Incorporating Macrofibers in Concrete Overlays [26]

In earlier practices, many engineers relied on experience when determining the type and quantity of fiber for pavement design. However, advances in testing standards and systematic laboratory evaluation have enabled more accurate assessment of FRC performance, supporting more informed decisions regarding fiber selection and dosage [27]. Even at low dosages with short fibers, as shown in Figure 2.15, fibers can improve load transfer, reduce crack growth, and enhance fatigue resistance compared to plain concrete [25]. In practice, the use of fibers is particularly appropriate for bonded concrete overlays with thicknesses of 10 cm (4 inches) or less [15]. In such applications, only structural-grade fibers should be used, as they are designed to improve concrete toughness and post-cracking behavior. The selected structural fiber should provide a residual strength of at least 20 percent to be considered effective. However, current evidence is insufficient to recommend the use of fibers in BCOA systems solely for the purpose of increasing panel size.

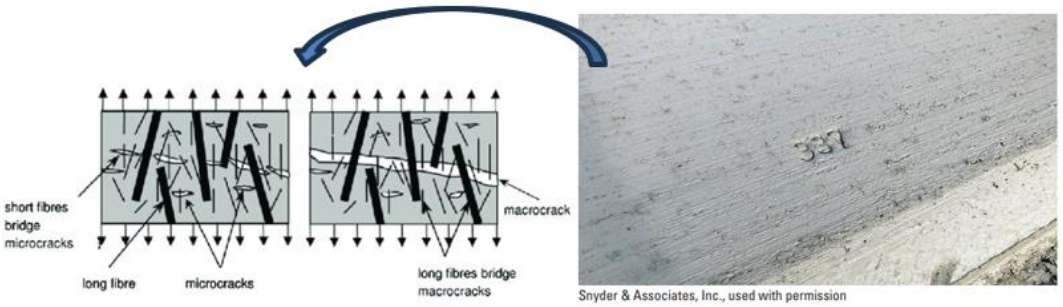

Figure 2.15 Short fibers enhance tensile strength by bridging microcracks; long fibers improve ductility by bridging macrocracks [14,28,29]

On the other hand, bonded concrete overlays are not suitable for all pavement conditions. Their application is limited in cases where asphalt pavements exhibit severe structural distresses, stripping, or lack adequate base and subbase support. Similarly, bonded overlays are not recommended for composite pavements with significant structural deterioration, poor drainage conditions, subgrade instability, or delamination issues. In such scenarios, full-depth reconstruction or alternative rehabilitation strategies should be considered to ensure long-term pavement performance and safety [14].

Although BCOA systems can be designed using various pavement analysis tools, BCOA-ME, developed by the University of Pittsburgh, stands out as the most effective and user-oriented option. This is primarily because it is specifically customized for bonded overlay applications, unlike other tools that are more general in scope. BCOA-ME is a specialized mechanistic-empirical software developed for the design of bonded concrete overlays on asphalt pavements. It incorporates key design parameters such as traffic loading, subgrade stiffness, fiber options, joint spacing, and existing asphalt condition to determine the required overlay thickness with accuracy. In addition to BCOA-ME, several other pavement design tools are commonly used in practice—such as Pavement ME, AASHTOWare, PAVEXpress, and other custom-developed software by individual state agencies. While these tools provide broader design capabilities for new rigid and flexible pavements, BCOA-ME remains the only widely adopted tool dedicated exclusively to bonded overlay design, offering greater accuracy and relevance for this application.

CHAPTER 3

METHODOLOGY

This chapter outlines the methodology followed to evaluate bonded concrete overlay designs on asphalt pavements using the BCOA-ME software developed by the University of Pittsburgh. The study aims to simulate and analyze various pavement scenarios in different regions of Türkiye by considering a wide range of input parameters, including traffic loads, subgrade conditions, existing asphalt layer properties, climate data, fiber reinforcement levels, and joint spacing configurations. A total of 1,440 design combinations were generated to reflect realistic field conditions in ten selected cities, each representing a distinct climatic zone. The results are used to develop recommended overlay thickness charts and to assess the influence of critical design variables on performance.

3.1 Design Requirements

To ensure practical applicability, this study considers the implementation of BCOA systems across ten provinces in Türkiye, each selected to represent distinct climatic conditions. The selected provinces—Afyonkarahisar, Erzurum, Eskişehir, İstanbul, İzmir, Kayseri, Konya, Mersin, Rize, and Şanlıurfa—capture a wide range of environmental variability, from coastal and humid regions to continental and arid zones. The analysis aims to propose customized overlay thickness designs for each city by accounting for subgrade quality, traffic volume, climate conditions, and other site-specific parameters. This location-based approach allows for the development of regionally optimized BCOA solutions that reflect real-world challenges and performance expectations.

A 20 years service life was selected to reflect typical performance expectations across the provinces. The study considered three subgrade quality levels (poor, moderate, and good), four levels of Average Annual Daily Traffic (AADT) to represent traffic volume ranges (low, low-moderate, moderate-high, and high), and a C30/37 concrete strength class. The reliability coefficient was consistently set at 85%, and the

maximum allowable cracked slab percentage was limited to 15% in accordance with GDH project demands and also given the increasing preference for fiber reinforcement in thin concrete overlay applications, synthetic fiber was incorporated at three dosages (0, 2.5, and 3.5 kg/m³) to evaluate its impact on overlay design. Joint spacings of 1x1 m (3x3 ft) and 2x2 m (6x6 ft) were also included in the analysis. Moreover, the condition of the existing asphalt pavement where the overlay will be applied was categorized into two levels: moderate (adequate) and severe (marginal). Accordingly, the percentage of transverse cracks on the existing pavement was taken into consideration in the analysis. The variable parameters used in the analysis are summarized in Table 3.1, resulting in a total of 1440 idealized design scenarios.

Table 3.1 Design variable values entered into the BCOA-ME Design Program.

Concrete Strength Class	C30/37			
Design Life	20 years			
Slab Percentage	15%			
Reliability	85%			
Percent Trucks %	Low Traffic =3.3	Low-Moderate Traffic=16	Moderate-High Traffic=25	High Traffic =50
Calculated ESAL values	~5 million	~30 million	~50 million	~100 million
Composite Modulus of Subgrade Reaction, k-value (Mpa/m)	Good=95 (350 pci)	Moderate=41 (150 pci)	Poor=14 (50 pci)	
Fiber Content (kg/m^3)	0 (0 lb/yd^3) 0%	2.50 (4 lb/yd^3) ~0.25%	3.50 (6 lb/yd^3) ~0.5%	
Existing HMA Performance	Adequate		Marginal	
Joint Spacing (m)	1x1 (3x3 ft) (Small Slab)		2x2 (6x6 ft) (Large Slab)	

3.2 Selection of Study Locations

Many aspects were considered while choosing the study locations, including varying climatic conditions, soil properties, environmental impacts, and vehicle composition, in order to create a provincial selection matrix that would reflect Türkiye overall. Cities were chosen with care to represent the average of each climatic class. The research also includes cities close natural ports, border crossings, or logistical sites, as well as cities on the international road network or rail freight transit, as truck traffic is predicted to increase in the future. Ten distinct provinces across Türkiye were selected as research regions based on a range of factors, including climatic variability. The Köppen–Geiger climate classification map of Türkiye, shown in

Figure **3.1**, illustrates these climate zones, while detailed climate data for the selected regions are provided in Section 3.4 [30].

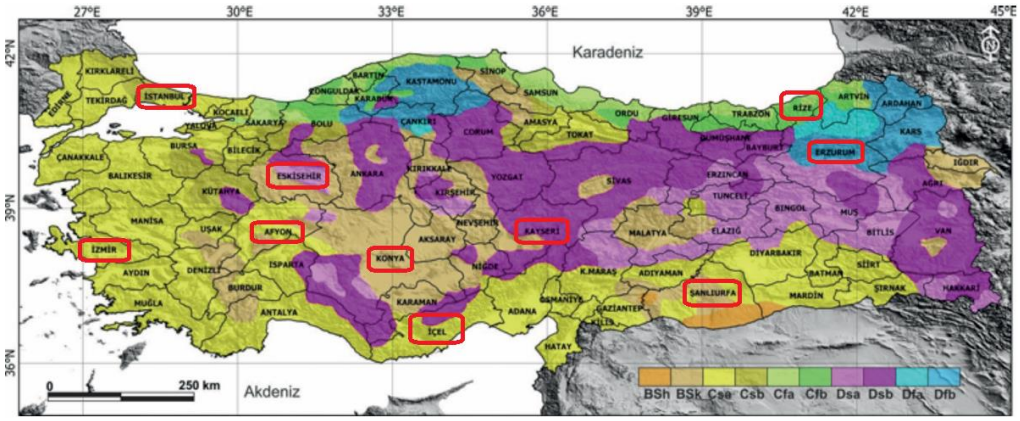

Figure 3.1 Köppen-Geiger climate type map of the Türkiye and selected provinces [31]

3.3 Traffic Volume Calculation

Traffic loading is a primary factor influencing pavement performance, as repeated axle loads induce structural fatigue over time. While determining the load effect of a single wheel or axle is relatively straightforward, estimating the cumulative impact of varying axle types and traffic volumes over a pavement's design life is considerably more complex. To simplify this, the concept of Equivalent Single Axle Load (ESAL) is widely used. The ESAL Eq.(3.1) represents the damage caused by a single standard axle load of 18 kip (80 kN) and serves as a common basis for comparing the effects of mixed traffic loading on pavement deterioration.

$$\mathrm{ESALdesign} = \mathrm{DD} \times \mathrm{LDF} \times \mathrm{Gf} \times \mathrm{ESALdaily} \times 365 \qquad \textbf{(3.1)}$$

In the Eq.(3.1), DD refers to the directional distribution factor, which represents the percentage of total traffic traveling in the design direction. For two-way traffic, a default DD value of 50% is typically used. LDF, or lane distribution factor, accounts for the distribution of traffic among lanes in the design direction. It is a function of the number of lanes and was obtained from Table 3.2. For single-lane roads, an LDF value of 100% was assumed.

Table 3.2 LDF factor [32]

Number of Lanes in each direction	Percent of 18-kip ESAL in design Lane
1	100
2	**80-100**
3	60-80
4	50-75

Based on the design inputs used in this study, the traffic parameters were defined as follows: design life (n) of 20 years, terminal serviceability (Pt) of 2.0, two lanes in each direction, and varying truck percentages of 3.3%, 16%, 25%, and 50%. The average daily traffic in one direction (ADT) was set at 30,000 vehicles, with an average daily truck traffic (ADTT) growth rate of 2%. A linear traffic growth rate was assumed, consistent with a major arterial road classification Table 3.3. For a linear growth model, the traffic growth factor (Gf) is calculated using the following Eq.(3.2):

$$\mathrm{Gf} = \mathrm{n} \times \left(1 + \mathrm{Gr}, \mathrm{ADTT} \times \frac{\mathrm{n}-1}{2}\right) \quad \textbf{(3.2)}$$

$$\mathrm{Gf} = 20 \times \left(1 + 0.02 \times \frac{20-1}{2}\right)$$

$$Gf = 23.8$$

Table 3.3 Axles per 1000 trucks for various types of roads. Taken from "Design of Concrete Pavement for City Streets (2002)".

Axle load (Kips)	**Axles per 1000 trucks**			
	Category LR	**Category 1**	**Category 2**	**Category 3**
Single axles				
4	846.15	1693.31	0.00	0.00
6	369.97	732.28	0.00	0.00
8	283.13	483.10	233.60	0.00
10	257.60	204.96	142.70	0.00
12	103.40	124.00	116.76	182.02
14	39.07	56.11	47.76	47.73
16	20.87	38.02	23.88	31.82
18	11.57	15.81	16.61	25.15
20	0.00	4.23	6.63	16.33
22	0.00	0.96	2.60	7.85
24	0.00	0.00	1.60	5.21
26	0.00	0.00	0.07	1.78
28	0.00	0.00	0.00	0.85

30	0.00	0.00	0.00	0.45
∑				**319.19**
Tandem axles				
4	15.12	31.90	0.00	0.00
8	39.21	85.59	47.01	0.00
12	48.34	139.30	91.15	0.00
16	72.69	75.02	59.25	99.34
20	64.33	57.10	45.00	85.94
24	42.24	39.18	30.74	72.54
28	38.55	68.48	44.43	121.22
32	27.82	69.59	54.76	103.63
36	14.22	4.19	38.79	56.25
40	0.00	0.00	7.76	21.31
44	0.00	0.00	1.16	8.01
48	0.00	0.00	0.00	2.91
52	0.00	0.00	0.00	1.19
∑				**572.34**

For Major Arterial Road Category have choosen '3' in Table 3.3 [2]. Eq.(3.3) through (3.12 present the step-by-step calculations of ESAL values for the low, low-moderate, moderate, and high traffic categories.

$$\text{ESALsdaily} = \text{NR} \times \text{LEF} \quad \textbf{(3.3)}$$

NR is the number of repetitions for a specific axle load per day

$$NR = \left(\frac{ADTT}{1000} \times Axles\ per\ 1000\ trucks\right) \quad \textbf{(3.4)}$$

$Axles\ per\ 1000\ trucks = 319.19 + 572.34 = 891.53$ (from Table 3.3)

$Axles\ per\ 1000\ trucks$ have been calculated below <u>single axle</u> for road category 3.

$$ADTT = \left(ADT \times \frac{Percent\ Trucks}{100}\right) \quad \textbf{(3.5)}$$

$ADTT\text{low}=30000\times3.3/100=990$

$ADTT\text{low-moderate}=30000\times16/100=4800$

$ADTT\text{moderate-high}=30000\times25/100=7500$

$ADTT\text{high}=30000\times50/100=15000$

$$NR = \left(\frac{\text{ADTT}}{1000} \times Axles\ per\ 1000\ trucks\right) \quad \textbf{(3.6)}$$

$$NR\ (low) = \frac{990}{1000} * (319) = 316$$

$$NR\ (low - moderate) = \frac{4800}{1000} * (319) = 1531$$

$$NR\ (moderate - high) = \frac{7500}{1000} * (319) = 2393$$

$$NR\ (high) = \frac{15000}{1000} * (319) = 4785$$

$$\text{LEF} = \left(\frac{\text{W18}}{\text{Wx}}\right) \quad \textbf{(3.7)}$$

In Eq.(3.8), L_x refers to the axle loading, 18 kips. L_2 is the weight of the axle (1 for single axle and 2 for tandem axle) is taken 1, also G_t is the growth rate and is given by Eq.(3.9) and Eq.(3.10). As seen in Eq.(3.11), βx is a constant to reflect the current loading in kips, x. $\beta_x = \beta_{18}$ for x = 18 kips. For each loading x, Wx is the number of 18-kip ESALs, and for x = 18 kips, $Wx = W18$ and also Eq.(3.12) is used to determine Wx:

$$Log(Wx) = 5.908 - 4.62\ log(Lx + L2) + 3.28log(L2) + \left(\frac{Gt}{\beta x}\right) - \frac{Gt}{\beta 18} \quad \textbf{(3.8)}$$

$$Gt = log\left(\frac{4.5 - Pt}{4.5 - 1.5}\right) \quad \textbf{(3.9)}$$

$$Gt = \log\left(\frac{4.5 - 2}{4.5 - 1.5}\right) \rightarrow Gt = -0.079 \quad \textbf{(3.10)}$$

$$\beta_x = 1 + \frac{3.63(L_x + L_2)^{5,2}}{(h_{PCC}+1)^{8.46} L_2^{3.52}} \rightarrow \beta_{18} = 1 + \frac{1.62\ (10)^7}{(h_{PCC}+1)^{8.46}} \quad \textbf{(3.11)}$$

Where h_{PCC} is the PCC thickness, in inch and for being,

$Wx = W18$, LEF=1, so $NR = ESALsdaily$ **(3.12)**

$ESALsdaily$ low= 316

$ESALsdaily$ low-moderate= 1531

$ESALsdaily$ moderate-high= 2393

$ESALsdaily$ high= 4785

$ESAL$design low= ~5 million from Eq.(3.1)

$ESAL$design low-moderate = ~30 million from Eq.(3.1)

$ESAL$design moderate-high = ~50 million from Eq.(3.1)

$ESAL$design high = ~100 million from Eq.(3.1)

3.4 Climate

The annual average temperature data for each city were determined by matching their climatic conditions to the corresponding regions on the AMDAT (Annual Mean Daily Average Temperature) map of the United States, seen in Figure 3.2 [30]. Based on this comparison, the assigned AMDAT zones are as follows: Afyonkarahisar, Erzurum, Eskişehir, Kayseri, and Konya correspond to Zone 3; İstanbul and Rize to Zone 4; İzmir to Zone 5; and Mersin and Şanlıurfa to Zone 6.

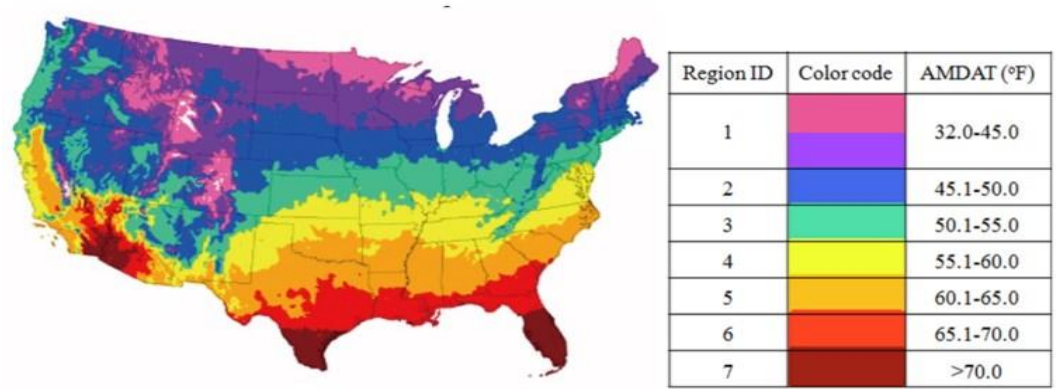

Figure 3.2 Map of AMDAT Region [5]

The average daily solar radiation data for each city were determined by identifying the corresponding regions based on the reference in [2,33]. According to this

classification, seen in Figure 3.3, Afyonkarahisar, Kayseri, Konya, Mersin, and Şanlıurfa fall into Region 3, while Erzurum, Eskişehir, İstanbul, İzmir, and Rize correspond to Region 4.

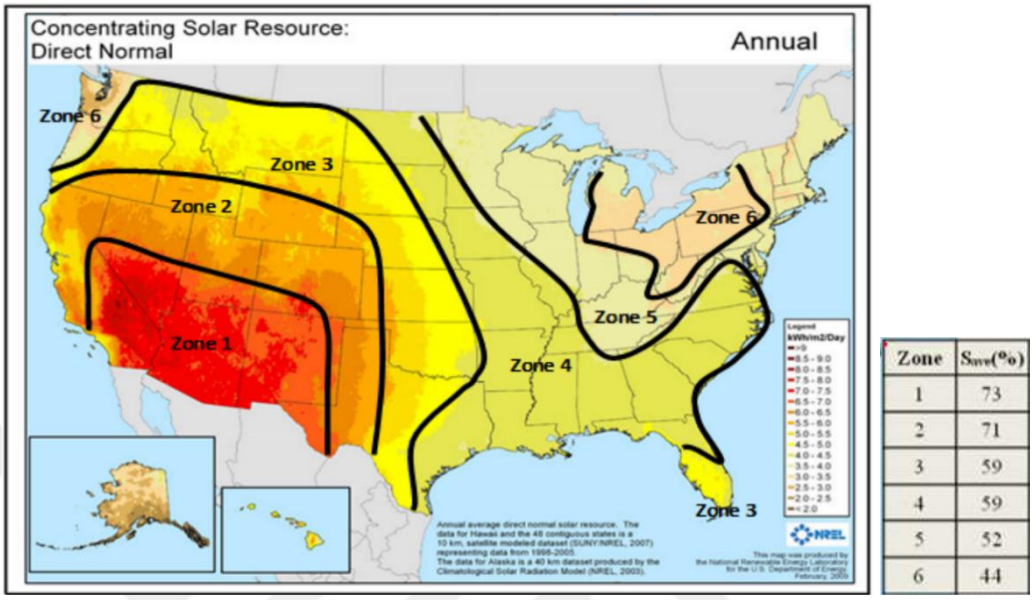

Zone	S_{ave}(%)
1	73
2	71
3	59
4	59
5	52
6	44

Figure 3.3 Annual concentrating solar resource map of USA [34]

In addition to the stress caused on by traffic loading, the temperature differential causes the slab to curl and produces environmental stress. This environmental stress must be calculated using a linear temperature gradient in the structural models for whitetopping slabs that are currently available. The linear temperature gradient cannot provide an appropriate estimation of environmental stress because the temperature change across the slab is nonlinear. Therefore, it is suggested that the environmental stress be characterized by the effective equivalent linear temperature gradient (EELTG).

The Enhanced Integrated Climatic Model (EICM) was then used to calculate the nonlinear temperature gradient for each project on an hourly basis while taking various whitetopping structures into account. Based on strain equivalence, the hourly nonlinear temperature gradients were then transformed into hourly equivalent linear temperature gradients (ELTGs) [35].

Ultimately, the EELTG was identified as the equivalent linear temperature gradient that causes the same amount of damage over the course of the design life as if hourly linear temperature gradients were applied. Here, damage may result from faulting or fatigue, and each is assessed using the models outlined below. As a result, distinct EELTGs are created for the two failure types (cracking and faulting). The EELTG and the climatic and structural characteristics of the PCC overlay for both faulting and fatigue were shown to be statistically related based on the database. The following Eq.(3.13) through (3.16) provide the corresponding relations for fatigue and faulting for various slab sizes [34,36].

As a result of the analyses and given that the BCOA-ME software is configured exclusively for climate stations within the United States, a matching process was conducted to associate the selected Turkish provinces with the most similar U.S.-based climate stations. This approach follows the methodology proposed by Öztürk et al. (2019), which offers a comprehensive framework for aligning regional climate conditions [30]. Table 3.4 presents the matched climate stations in the U.S. that best represent the climatic performance of the corresponding provinces in Türkiye.

Table 3.4 Similar climate stations belong to provincial regions [30].

Provincial Regions	Similar Climate Stations
Afyonkarahisar	Spokane, WA (24157)
Erzurum	Idaho Falls, ID (24145)
Eskişehir	Pullman/Moscow, WA (94129)
İstanbul	Sacramento, CA
İzmir	Marysville, CA (93205)
Kayseri	Price, UT. (93141)
Konya	Ogden, UT (24126)
Mersin	Burbank, CA (23152)
Rize	Crescent City, CA
Şanlıurfa	Safford, AZ (93084)

3.4.1 EELTG (ΔT) for Fatigue Cracking

For smaller slabs (joint spacing ≤ 4.5 ft (1.5m) × 4.5 ft (1.5m)), the $EELTG_{small\ slabs}^{fatique}$ is given by (R^2 adj = 0.640):

$$EELTG_{small\ slabs}^{fatique} = 0.534 - 0.0015644Latitude - 0.0009853Longitude - 0.00002145Elevation - 0.0067836S_{ave} + 0.15843L - 0.202627h_{HMA} - 0.00175066M_R \quad \textbf{(3.13)}$$

For mid-size slabs (joint spacing > 4.5 ft (1.5m) and ≤ 7 ft (2.0m), the $EELTG_{mid-size\ slabs}^{fatique}$ is given by (R^2 adj = 0.710):

$$EELTG_{mid-size\ slabs}^{fatique} = 0.85895 + 0.0046918Latitude + 0.0018581Longitude + 0.000003625Elevation - 0.0082567S_{ave} - 0.127695h_{HMA} + 0.00077175M_R \quad \textbf{(3.14)}$$

where, $EELTG$ - effective equivalent linear temperature gradient, °F/in. $Latitude$ - geographical latitude of the project location, degrees. $Longitude$ - geographical longitude of the project location, degrees. $Elevation$ - distance of the project location above sea level, ft. S_{ave} - annual mean percentage of sunshine, %. L - overlay slab size of PCC, m. h_{HMA} - HMA thickness, in. h_{pcc} - overlay thickness of PCC, in. M_R - modulus of rupture of PCC, psi, as seen in Eq.(3.13) and (3.14).

3.4.2 EELTG (ΔT) for Faulting

Small slabs (joint spacing ≤ 4.5 ft (1.5m)) are not examined for faulting for the above mentioned reasons. The EELTGs for medium-sized slabs (slabs with joint spacing ≤ 10 ft (3 m)) were computed as follows: $EELTG_{Mid-full}^{faulting}$ for joint activation through both the PCC and HMA layers, and $EELTG_{Mid-PCC}^{faulting}$ for joint activation through the PCC layer alone. Since shorter plates are insensitive, a constant value of **-1.5** was found to be sufficient to obtain accurate results [2].

3.4.3 Determination EELTG' Inputs

In addition to user-defined structural design inputs like the PCC overlay slab size, HMA layer thickness, and PCC modulus of rupture, the EELTG computation requires user-defined geographic inputs like latitude, longitude, and elevation. The yearly mean percentage of sunlight is also necessary, and Figure 3.3 provides common values based on geographic zones.

For some inputs, seasonal temperature variations across the country are also taken into account. To simplify this input, the region for the city of interest was selected from the annual mean daily temperature (AMDAT) map as shown in Figure 3.2.

EELTG, WETDAYS, Freezing Ratio (FR), and mean monthly nighttime mid-depth PCC temperature are also used in the faulting prediction model in Eq.(3.15) and Eq.(3.16). WETDAYS is the average number of days with precipitation over 0.1 in, while FR is the percentage of time the base layer or asphalt layer is less than 32 °F, reducing erodibility and faulting development. For WETDAYS (R^2 adj = 0.590) and FR:

$$\begin{aligned}\text{WETDAYS} = {} & -102.3 + 25.81 bSunZone + 2.063 AMDATZone \\ & - 1.216 Latitude + 0.3804 Longitude \\ & + 1.429 S_{ave}\end{aligned} \tag{3.15}$$

$$\begin{aligned}\text{FR} = {} & C_1 + C_2 h_{PCC} + C_3 h_{HMA} + C_4 AMDATZone + \\ & C_5 Latitude + C_6 Longitude + C_7 Elevation\end{aligned} \tag{3.16}$$

The coefficients $C_1 - C_7$ in Eq.(3.16) are functions of the sunshine zone as shown in Table 3.5.

Table 3.5 Freezing ratio regression coefficients

Sun. zone	C_1	C_2	C_3	C_4	C_5	C_6	C_7	R2 adj.
PCC-depth joint activation								
1	-87.1	-0.111	-0.140	-2.58	0.711	0.705	4.2E-04	0.699
2	73.21	-0.094	-0.281	-7.332	0.878	-0.551	-3.5E-03	0.607
3	80.4	-0.008	-0.136	-5.342	0.096	-0.563	7.4E-04	0.686
4	-53.71	-0.004	-0.106	-3.141	0.864	0.502	3.1E-03	0.920
5	-77.15	0.066	-0.218	-1.763	1.998	0.149	1.9E-03	0.922

6	-15.74	-0.017	-0.255	-2.072	1.821	-0.495	9.4E-04	0.840
Full-depth joint activation								
1	-146.78	-0.133	-0.324	-3.102	0.446	1.333	1.5E-03	0.680
2	84.51	-0.172	-0.770	-7.767	1.419	-0.776	4.0E-03	0.536
3	32.731	-0.030	-0.137	-5.659	0.072	-0.024	2.2E-04	0.697
4	32.731	-0.030	-0.137	-5.659	0.072	-0.024	2.2E-04	0.697
5	81.919	-0.010	-0.083	-7.967	-0.472	-0.302	3.6E-03	0.698
6	52.531	-0.247	0.003	-4.036	-0.940	0.217	-3.1E-03	0.636

3.5 Existing Structure HMA

The structural condition of the existing HMA pavement plays a crucial role in bonded concrete overlay performance, particularly in determining the support stiffness beneath the overlay. In the BCOA-ME framework, the HMA layer is categorized as either “adequate” or “marginal”, based on its fatigue cracking severity. According to Harrington (2008) and the MEPDG guidelines, HMA with 0–8% fatigue cracking is classified as adequate, while HMA with 8–20% fatigue cracking falls into the marginal category as shown in Table 3.6 [12]. These categories correspond to fatigue damage factors of 0.3 and 0.4, respectively, which are then used to reduce the dynamic modulus of the asphalt layer. A higher damage factor indicates a weaker support condition, which results in higher stress levels in the concrete overlay and consequently requires a thicker design to meet fatigue performance criteria.

Table 3.6 Influence of Existing HMA Pavement Condition on Modulus Reduction and Damage Factor

HMA Pavement Condition	Fatigue Cracking (%)	Damage Factor d<sub>AC</sub)	Modulus Reduction (%)	Interpretation
Adequate	0-8 %	0.3	5%	Structurally sound, minimal cracking
Marginal	8-20 %	0.4	12.5%	Moderate fatigue damage, reduced stiffness

For practical design purposes, the model assumes a 5% modulus reduction for adequate HMA and a 12.5% reduction for marginal HMA. These reductions significantly affect overlay stress distribution and deflection responses, making an accurate assessment of HMA condition essential for realistic overlay thickness design. The degraded modulus is ultimately used in calculating the composite k-value, which governs how the bonded system responds to loading and fatigue.

Since a post-milling HMA thickness of 6–7 cm is considered sufficient for bonded concrete overlays, this value was selected for the analysis. The stiffness of all layers beneath the asphalt is represented by the composite k-value. As shown in Table 3.7, subgrade support conditions were categorized as follows: poor (50 pci), moderate (150 pci), and good (350 pci). These k-values were used in the analysis to reflect varying subgrade qualities. Additionally, it was assumed that the existing HMA pavement contains transverse cracks.

Table 3.7 Composite Modulus of Subgrade Reaction, k-value [37]

Soil Type	**k (pci)**
Plastic clay	50-100
Silt and silty clay	100-200
Sand, clay gravel	200-300
Gravel	300-350
Crushed Stone (Subbase/Base)	350-450

Transverse cracks, as shown in Figure 3. 4, that run directly against the centerline of the pavement. Fatigue cracking (Figure 3. 5) is found in areas subjected to repeated traffic loadings (wheelpaths). It can appear as a series of cracks in the early stages of development. It ultimately transforms into different pattern [2].



(a) Non-deteriorated **(**1) **(b)** Deteriorated **(**2)

Figure 3. 4 Transverse cracking in an existing HMA pavement [2]



(a) Adequate (Non-Deteriorated) **(**1) **(b)** Marginal (Deteriorated) **(**2)

Figure 3. 5 Fatigue Severity Levels [2]

Figure 3. 6 illustrates several types of pavement distresses that can be effectively treated using a BCOA. Many of these surface-level distresses are typically eliminated during the milling process conducted before overlay placement.



Figure 3. 6 Typical Distresses Observed in Hot Mix Asphalt (HMA) Pavements [15]

The flowchart in Figure 3. 7 is a tool developed by the National Concrete Pavement Technology Center (CP Tech Center) that can be used for determining if a BCOA is a good rehabilitation alternative for a distressed HMA pavement.

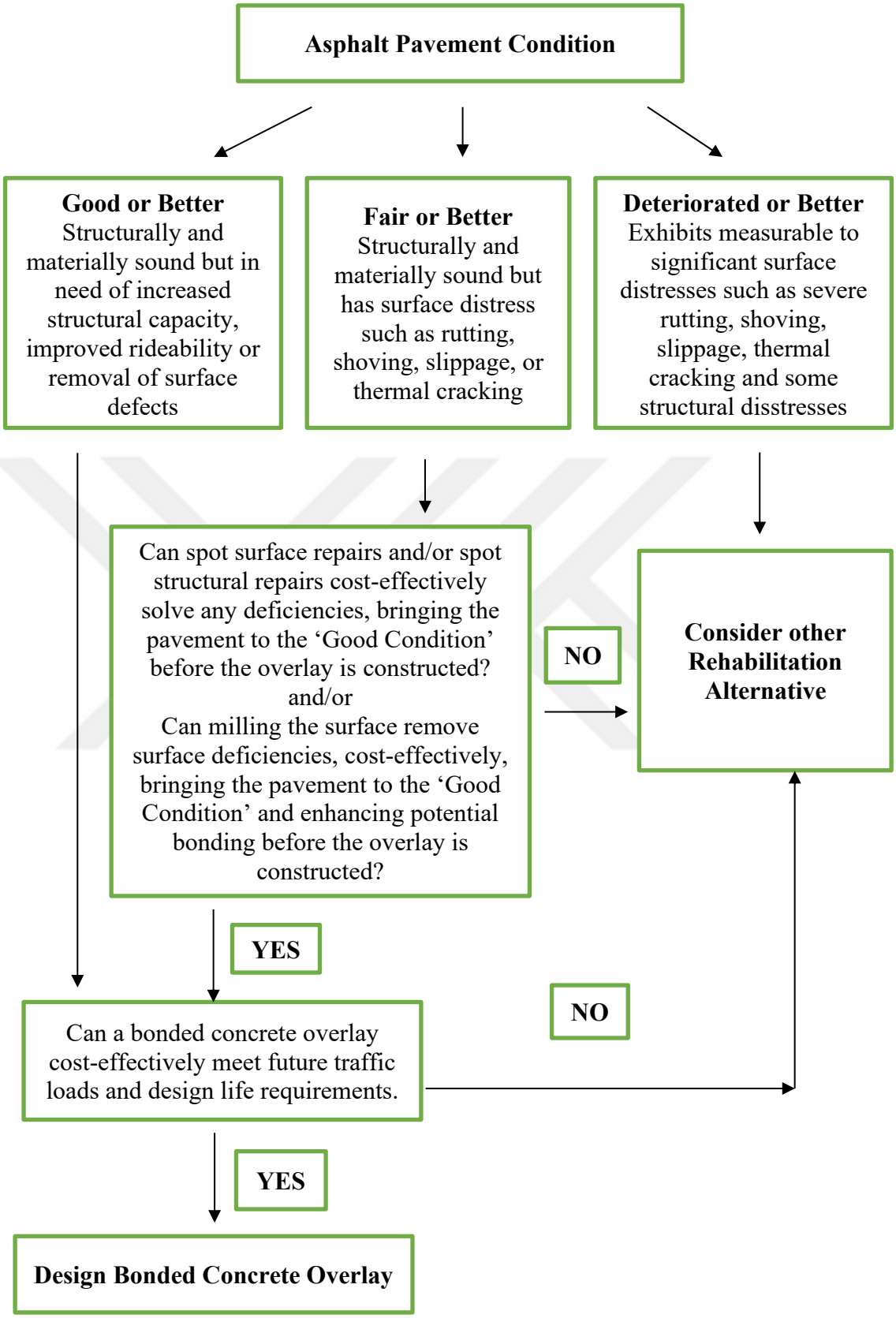

Figure 3. 7 Flowchart for Evaluating the Suitability of BCOA as a Rehabilitation Option [15]

According to the average of 482 data (Table 3.8) obtained from the General Directorate of Highways and Geopave Consulting in Türkiye, the percentage of aggregate passing the #200 sieve in the HMA mix (HMA P200) is 5.54%, the percentage of aggregate passing the #200 sieve in the layer immediately below the asphalt layers (Subbase P200) is 7%, the effective binder content by volume is 5% and the percentage of air voids in the HMA mix is 4.65%.

Table 3.8 Average values of HMA in Türkiye

Pavement Layer Type	P200 (%) [Spec,2023]	Effective Binder Content by Weight (%) [Spec,2023]	Air Voids (%) [Spec,2023]
HMA, Bitumen Base Course	4,93	4,14	4,51
HMA, Binder Course	5,02	4,43	4,69
HMA, Wearing Course-AC	5,76	4,98	4,13
HMA, Wearing Course-SMA	10,47	6,86	3,35
HMA, Average	5,54	4,61	4,65
Base & Subbase	7,00	[0-12]	

3.6 PCC Overlay Strength Properties

For the concrete overlay design, a C30/37 grade concrete was selected. The average 28-day flexural strength (three-point bending strength) was taken as 4.3 MPa (613 psi), and the estimated elastic modulus was assumed to be 32 GPa (~4,500,000 psi) [37]. The concrete thermal expansion coefficient, based on limestone aggregates, was taken as 3.8×10^{-6} /°C. The cement content was set at 325 kg/m³. Additionally, no dowel bars were included in the design, and a tied shoulder configuration was assumed for all scenarios [32].

Under axle loads, concrete pavements undergo bending, which generates both flexural and compressive stresses. In pavement design, flexural strength is the critical parameter because the ratio of applied flexural stress to flexural strength is significantly greater than that of compressive stress to compressive strength. As a result, flexural performance governs the structural design of concrete pavements. The flexural strength of concrete is typically evaluated using modulus of rupture (MOR) tests, which provide a measure of the material's resistance to bending failure [38].

3.7 Fiber Effect

The incorporation of fibers into concrete has been a widely adopted strategy to improve the material's tensile behavior, crack resistance, and post-cracking performance. Fibers bridge cracks and help distribute stress more evenly, thereby enhancing the ductility of concrete, especially under repeated loading. The type, length, and dosage of fibers influence the mechanical response, particularly in applications such as overlays, where cracking resistance is critical. Figure 3. 8 presents the tensile stress–strain behavior of normal concrete (NC), fiber-reinforced concrete (FRC), and ultra-high-performance fiber-reinforced concrete (UHPFRC). While NC fails immediately after first cracking, FRC provides improved load-carrying capacity beyond cracking through strain-softening behavior. UHPFRC further exhibits strain-hardening and multiple cracking, enabling it to sustain higher tensile stresses and strains, which is highly beneficial in pavement and structural applications requiring higher performance.

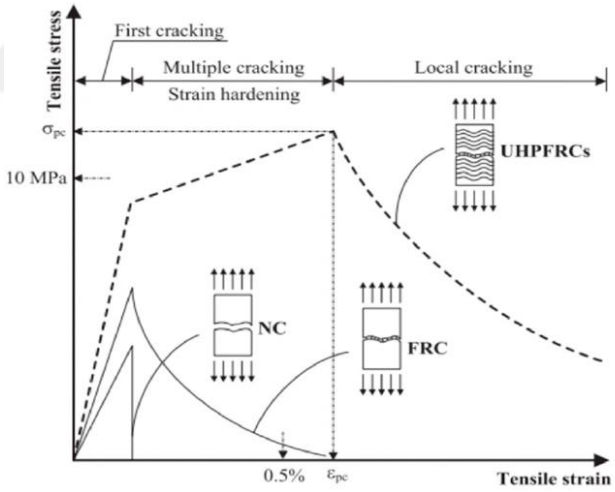

Figure 3. 8 A comparison of normal, FRC (fiber reinforced) and ultra high performance FRC types of concrete in tensile stress and strain [39]

Fiber reinforcement technology has long been applied in pavement engineering, initially focusing on steel macrofibers to enhance fatigue life. However, limitations such as high dosage requirements, corrosion concerns, increased material costs, and limited design guidance hindered widespread adoption. Synthetic microfibers introduced in the 1980s addressed early-age plastic shrinkage but lacked structural benefits. In contrast, re. Despite advancements in testing standards and design

guidance, broader adoption is still challenged by knowledge gaps among engineers and practitioners regarding fiber types, dosage, performance testing, and construction adjustments. Addressing these issues is essential for integrating macrofibers into structural overlay designs effectively [26].

FRC has been increasingly used in pavement applications, not only for new construction but also for maintenance (e.g., patching), rehabilitation (e.g., bonded overlays), and reconstruction. Over the past decade, the use of FRC in BCOA for minor rehabilitation has grown significantly, especially in thin sections ranging from 7.5 to 15 cm. According to the National Concrete Overlay Explorer, as of April 2018, there were 89 documented FRC overlay projects in the U.S., with 54% classified as BCOA and most constructed after 2000. Field studies, including a survey in Illinois, have shown that macrofibers enhance structural performance in ultra-thin whitetopping (UTW) overlays by improving joint load transfer and overall slab durability. Even in cases where cracking was observed, overlays reinforced with macrofibers maintained good serviceability and ride quality. Based on falling weight deflectometer (FWD) data, macrofibers are recommended for all UTW applications ≤10 cm, and even for thicker sections up to 15 cm. For light-duty applications like parking lots, minimum fiber dosages are sufficient, while for roadways, a residual strength (R_{150}) greater than 20% is recommended. For pavements over distressed asphalt or subjected to heavy truck traffic or weak support layers, higher macrofiber dosages—up to 4.5 kg/m^3 (7.5 lb/yd^3)—are advised to reduce crack deterioration and enhance continuity between adjacent slabs [40].

The inclusion of macrofibers in concrete overlay design enhances post-cracking performance and fatigue resistance, both of which are critical for extending pavement life under repetitive traffic loads. While the flexural strength of FRC may appear similar to that of plain concrete in conventional tests, it is the residual strength specifically R_{150} that captures the true benefit of macrofibers in slab behavior [41]. This residual strength is measured using ASTM C1609, a standard test that evaluates the load-deflection response of FRC beams in third-point loading as shown in Figure 3. 9.

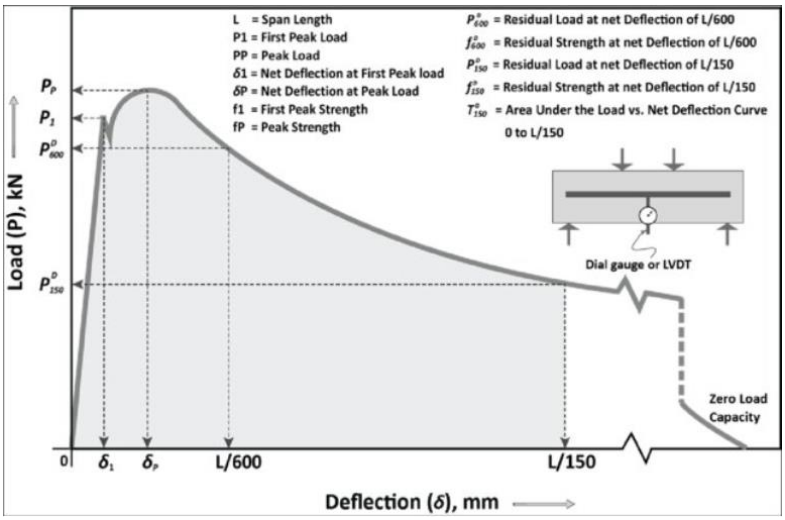

Figure 3. 9 ASTM C1609 typical load-deflection graphs and necessary parameters for calculating [44]

For overlay design purposes, the effective flexural strength (MoR+R_{150}) is proposed as a more accurate input than traditional flexural strength. It is calculated as the sum of the actual concrete flexural strength (MoR) and the residual strength (R_{150}) at net deflection of L/150. A minimum R_{150} value of 20%—corresponding to between 0.7 MPa and 1.0 MPa (100 and 150 psi) is recommended for FRC overlays [27]. The effective flexural strength is then used to compute the stress ratio (S_R), as seen Eq.(3.17), where σ_{design} is the tensile stress induced in the overlay. This ratio is applied in fatigue analysis using the same framework as that for plain concrete pavement design, thereby allowing macrofibers to be systematically incorporated into overlay thickness and performance predictions [22,27,41,42].

$$S_R = \frac{\sigma_{design}}{(1+R_{150})\times M_R} \quad \textbf{(3.17)}$$

In this study, the influence of fiber reinforcement on BCOA design was evaluated by comparing both unreinforced and fiber-reinforced scenarios using fiber dosages of 2.5 and 3.5 kg/m³. To clearly illustrate the effect of fiber inclusion, a representative case was calculated step-by-step in Sections 3.7.1 through 3.7.4 and also following Eq.(3.13) through (3. 35) covering the determination of design tensile stresses-σ_{design}, stress ratios-S_R, and the corresponding number of load cycles to fatigue failure (Nf). The same computational process was applied to all case scenarios using the BCOA-ME software [2]. This methodology enabled a direct comparison of how varying fiber

dosages influence the structural performance and fatigue resistance of the overlay system. In following section, small slab calculations are shown for demonstration equations taken from BCOA-ME theory manual [33].

3.7.1 Design Stress for Slabs Joint Spacing ≤ 4.5 ft (Small Slab)

$$log(\sigma_{18}) = 5.025 - 0.465\log(k) + 0.686\,log\left(\frac{L}{l_e}\right) - 1.291\log(l_e) \quad \textbf{(3.18)}$$

In Eq.(3.18), σ_{18} refers to the maximum stress in the PCC overlay under 18-kip wheel load in psi. k is the modulus of subgrade reaction, 150 psi/in. L is the slab length (assuming square slabs), le is the effective radius of relative stiffness, also h_{HMA} and h_{PCC} are the thicknesses of HMA after milling and PCC overlay respectively in inch. Also E_{HMA} is the HMA modulus, psi. Besides, in Eq.(3.19) through (3.21); Im is the moment of inertia and NA is the neutral axis of the composite pavement.

$$NA = \frac{(E_{PCC}h_{PCC}^2)/2+(E_{HMA}h_{HMA})(h_{PCC}+\frac{h_{HMA}}{2})}{E_{PCC}h_{PCC}+E_{HMA}h_{HMA}} \quad \textbf{(3.19)}$$

$$l_e = \left[\frac{Im}{(1-0.15^2)\times k}\right]^{0.25} \quad \textbf{(3.20)}$$

$$Im = \frac{E_{PCC}h_{PCC}^3}{12} + E_{PCC}h_{PCC}\left(NA - \frac{h_{PCC}}{2}\right)^2 + \frac{E_{HMA}h_{HMA}^3}{12} + E_{HMA}h_{HMA}\left(h_{PCC} - NA + \frac{h_{HMA}}{2}\right)^2 \quad \textbf{(3.21)}$$

$$(\sigma_T) = 28.037 - 3.496(CTE\ \times \Delta T) - 18.382 \times \left(\frac{L}{l_e}\right) \quad \textbf{(3.22)}$$

In Eq.(3.22), σT is the critical temperature-induced stress, CTE is the coefficient of thermal expansion for limestone is 3.8 $\times 10^{-6}$ in/in/°F, ΔT is the effective equivalent linear temperature gradient (EELTG), as seen in Eq.(3.23), °F/in. h_{PCC} is 4 in and h_{HMA} is 3 in this project. $E_{PCC}\ is\ 4641206$ and $E_{HMA}\ is\ 450000$ (max), in psi.

Additionally, L = 3 ft =36 in (assuming square slabs). According to this values;

NA = 2.24 from Eq.(3.19)

Im = 41,116,289 in⁴ from Eq.(3.21)

l_e = 23.01 in from Eq.(3.20)

σ_{18} = **245 psi** from Eq.(3.18)

$$\Delta T = EELTG_{small\ slabs} = 0.534 - 0.0015644Latitude - 0.0009853Longitude - 0.00002145Elevation - 0.0067836S_{ave} + 0.15843L - 0.202627h_{HMA} - 0.00175066M_R \quad \textbf{(3.23)}$$

For case;

Latitude= 47.37 °

Longitude= -117.32 °

Elevation= 2384 ft

S_{ave} = is the annual mean percentage of sunshine, % = 59 from Figure 3.3

$\Delta T = EELTG_{small\ slabs}$ = -0.572 from Eq.(3.23)

This negative result indicates that under the given environmental and design conditions, the early-entry longitudinal temperature gradient effect is not favorable for fatigue performance in small slabs-which is typical when high stiffness and environmental stress combine.

$$(\sigma_T) = 28.037 - 3.496(3.8 \times 10^{-6} \times -0.572) - 18.382 \times \left(\frac{165}{65.41}\right)$$

$\boldsymbol{\sigma_T}$ = **-0.72 psi** from Eq.(3.22)

The calculated temperature-induced stress in the concrete overlay was found to be relatively low, primarily due to the combination of a small temperature gradient, a short slab length, and the use of concrete with a low coefficient of thermal expansion, typical for limestone aggregates. These conditions result in minimal internal strain due to thermal effects. Additionally, small slabs inherently limit the development of significant temperature-induced bending stresses because of their reduced dimensions and restrained thermal movement.

As a side note, in bonded concrete overlay design, especially when using tools like BCOA-ME, the influence of temperature is typically accounted for using empirical indices such as the $EELTG_{small\ slabs}$. While it might seem logical to use direct temperature gradient data—such as daily, monthly, or annual mean values—the EELTG parameter functions as a representative indicator of how thermal effects contribute to slab fatigue, based on regional climate variables like latitude, elevation, sunshine percentage, and slab geometry. This approach avoids the complexity and variability of real-time or site-specific temperature measurements while still capturing their long-term structural effects through regression-based modeling. Although using measured thermal gradients would provide higher accuracy, the current practice simplifies input requirements and ensures consistency in design while remaining conservative in safety estimations.

The design stress (σ_{design}) is the sum of the adjusted load- and temperature-induced stresses, as seen in Eq.(3.24). $Fstress$ is the stress adjustment factor. As there is no performance data available, the stress adjustment factor can be taken as 1.5.

$$\sigma_{design} = \sigma_{18} \times F_{stress} + \sigma_T \quad \textbf{(3.24)}$$

$$\sigma_{design} = 245 \times 1.5 - 0.72$$

$$\boldsymbol{\sigma_{design}} = \mathbf{367\ psi}$$

The number of permitted load repetitions, Nf, is calculated using the fatigue equation established by Riley et al. (2005), as seen in Eq.(3.25) [43]. *SR* is the stress ratio and *R* is the reliability taken as 85%.

$$log(N_f) = \left(\frac{-SR^{-10.24}\, log(R)}{0.0112}\right)^{0.217} \quad \textbf{(3.25)}$$

For whitetopping projects, structural fibers may be used, especially if the PCC overlay thickness is less than or equal to 4 inches. This design uses the fiber contribution accounting approach created by the Illinois Center for Transportation [22]. Because fiber reinforced concrete (FRC) has a higher residual strength ratio, adding fiber improves the performance of the whitetopping. By adding the residual strength to the modulus of rupture, it is predicted that the improved performance of the FRC

whitetopping can be explained. Consequently, by adding residual strength to MR, the equivalent stress ratio for the FRC whitetopping can be written as equation below.

$$s_R = \frac{\sigma_{design}}{(1+R_{150}^{150})\times M_R} \quad \textbf{(3.17)}$$

The residual strength ratio, or R_{150}^{150}, describes how much fiber reinforcement contributes to concrete mixtures. M_R is the modulus of rupture of the PCC overlay,seen in Eq.(3.26), psi and fc' is the compressive strength of the PCC, psi.

$$M_R = 2.30 f_c^{\prime\frac{2}{3}} \quad \textbf{(3.26)}$$

M_R=2.30 X $4350^{2/3}$ = 613

$$v_{fiber}^{input} = \frac{w_{fiber}}{s_G \times 62.4 \times 27} \quad \textbf{(3.27)}$$

v_{fiber}^{input} is the fiber's volume content, %

w_{fiber} is the fiber's weight, lb/yd^3

s_G is the fiber's specific gravity

The Incremental Stress Factor (ISF) is used to estimate the stress ratio for fiber-reinforced concrete based on the input fiber volume, as seen in Eq.(3.28). It considers the volumetric content of fibers, as well as the minimum and maximum recommended fiber dosages. The ISF quantifies how different fiber volumes influence the stress factor and helps define threshold values corresponding to each fiber content level, as presented in Table 3.9.

$$ISF = \frac{v_{fiber}^{input} - v_{min}}{v_{max} - v_{min}}(Bmax - Bmin) + Bmin \quad \textbf{(3.28)}$$

Where v_{fiber}^{input}, v_{min} and v_{max} are the input fiber volume, minimum and maximum absolute volume fraction, %. Also $Bmin$ and $Bmax$ are the stress factors associated with minimum and maximum fiber volumes.

Table 3.9 Experimentally determined limit values of stress factors for different types of fibers.

Fiber Type	Specific gravity	Absolute volume fraction, %		Stress factor	
		VMIN	***VMAX***	***BMIN***	***BMAX***
None	1.0	100.0	-	1.00	1.00
Synthetic Structural Fibers	0.92	0.194	0.477	1.24	1.39

The initial estimate for an analogous stress ratio factor for a particular fiber type is the trial safety factor SF^{Trial} in Eq.(3. 29). A safety element in the stress factor is taken into account by this consideration:

$$SF^{Trial} = ISF - SF_{fiber}^{0} \quad \textbf{(3. 29)}$$

SF_{fiber}^{0} is a arbitrary safety factor, 0.05. Beside, in Eq.(3. 30) through (3. 33); SF_{min} and SF_{max} are the minimum and maximum allowed factors, SF^{Final} is the equivalent stress ratio factor and R_{150}^{150} is contribution of the concrete's reinforcement.

$$SF_{min} = \begin{cases} 1.0\,,\ V_{fiber}^{input} < V_{min} \\ SF^{Trial}, V_{fiber}^{input} \geq V_{min} \end{cases} \quad \textbf{(3. 30)}$$

$$SF_{max} = \min(\ SF^{Trial}, B_{max}) \quad \textbf{(3. 31)}$$

$$SF^{Final} = \max(\ 1.0, \min\ (\ SF^{Trial}, B_{max})) \quad \textbf{(3. 32)}$$

$$R_{150}^{150} = SF^{Final} - 1 \quad \textbf{(3. 33)}$$

3.7.2 No Fiber Condition

$v_{fiber}^{input} = \frac{0}{s_G \times 62.4 \times 27}$= 0 from Eq.(3.27)

$ISF = \frac{0-1}{0-1}(1-1) + 1$= 1 from Eq.(3.28)

$SF^{Trial} = 1 - 0.05 = 0.95$ from Eq.(3. 29)

$SF_{min} = \begin{cases} 1.0\ , V_{fiber}^{input} < V_{min} \\ SF^{Trial}, V_{fiber}^{input} \geq V_{min} \end{cases}$; $SF_{min} = 1$ from Eq.(3. 30)

$SF_{max} = \min(\ 0.95,1)$; $SF_{max} = 1$ from Eq.(3. 31)

$SF^{Final} = \max(\ 1.0, \min\ (\ 0.95, 1))$; $SF^{Final} = 1$ from Eq.(3. 32)

$R_{150}^{150} = 1 - 1 = 0$ from Eq.(3. 33)

$\sigma_{design-smallslabs} = 367$ psi from Eq.(3.24)

$s_{R(small\ slabs)} = \frac{367}{(1+0)\times 613} = 0.60$ from Eq.(3.17)

R= reliability= 85% =0.85

$\boldsymbol{N_{fsmallslabs}}$ = ~ **43,500** from Eq.(3.25)

3.7.3 Fiber Volume 2.5 kg/m³ (4.0 lb/$\boldsymbol{yd^3}$)

$v_{fiber}^{input} = \frac{4}{0.92 \times 62.4 \times 27}$= 0.0025 (0.25%) from Eq.(3.27)

$ISF = \frac{0.0025-0.194}{0.477-0.194}(1.39 - 1.24) + 1.24$= 1.138 from Eq.(3.28)

$SF^{Trial} = 1.138 - 0.05 = 1.088$ from Eq.(3. 29)

$SF_{min} = \begin{cases} 1.0\ , & 0.0025 < 0.194 \\ 1.088, & 0.0025 \geq 0.194 \end{cases}$; $SF_{min} = 1$ from Eq.(3. 30)

$SF_{max} = \min(\ 1.088,1.39)$; $SF_{max} = 1.088$ from Eq.(3. 31)

$SF^{Final} = \max(1.0, \min(1.088, 1.39))$; $SF^{Final} = 1.088$ from Eq.(3. 32)

$R_{150}^{150} = 1.088 - 1 = 0.088$ from Eq.(3. 33)

$s_{R(small\ slabs)} = \frac{367}{(1+0.088)\times 613} = 0.55$ from Eq.(3.17)

$\boldsymbol{N_{fsmallslabs}}^{=}$ ~**425,000** from Eq.(3.25)

3.7.4 Fiber Volume 3.5kg/m³ (6.0 lb/yd^3)

$v_{fiber}^{input} = \frac{6}{0.92\times 62.4\times 27} = 0.004$ (0.4%) from Eq.(3.27)

$ISF = \frac{0.004-0.194}{0.477-0.194}(1.39 - 1.24) + 1.24 = 1.140$ from Eq.(3.28)

$SF^{Trial} = 1.140 - 0.05 = 1.09$ from Eq.(3. 29)

$SF_{min} = \begin{cases} 1.0, & 0.004 < 0.194 \\ 1.09, & 0.004 \geq 0.194 \end{cases}$; $SF_{min} = 1$ from Eq.(3. 30)

$SF_{max} = \min(1.09, 1.39)$; $SF_{max} = 1.09$ from Eq.(3. 31)

$SF^{Final} = \max(1.0, \min(1.09, 1.39))$; $SF^{Final} = 1.09$ from Eq.(3. 32)

$R_{150}^{150} = 1.09 - 1 = 0.09$ from Eq.(3. 33)

$s_{R(small\ slabs)} = \frac{367}{(1+0.09)\times 613} = 0.54$ from Eq.(3.17)

$\boldsymbol{N_{fsmallslabs}}^{=}$ ~**750,000** from Eq.(3.25)

In this particular case, the estimated fatigue life (Nf) was approximately 43,500 load cycles when no fibers were used. With the inclusion of fibers at a dosage of 2.5 kg/m³, Nf increased to approximately 425,000, and further to around 750,000 with 3.5 kg/m³. These results clearly demonstrate that the use of fiber reinforcement significantly enhances the fatigue performance of bonded overlays at the same slab thickness.

However, when these Nf values are compared against the cumulative ESALs expected over a 20-year design period, they fall short of the required performance. Consequently, the design must be re-evaluated using a thicker overlay—greater than the 4-inch (10 cm) thickness assumed in this scenario. These recalculations are carried out automatically within the BCOA-ME software, while this section aims only to illustrate the underlying computational steps and highlight the influence of input variables on fatigue life.

3.8 Reflective Cracking Potential

Reflective cracking is a critical performance concern in bonded concrete overlays, particularly when applied over existing asphalt pavements with underlying cracks or structural fatigue. These cracks can propagate upward into the new overlay due to a combination of load-induced stresses and temperature fluctuations. In bonded overlays, the interface between the concrete and asphalt behaves monolithically, transferring stress directly and increasing the potential for crack reflection if the underlying pavement is in poor condition. BCOA systems are particularly vulnerable when applied over asphalt pavements that exhibit severe fatigue cracking, stripping, or poor support conditions. While BCOA offers a structural upgrade, its effectiveness depends largely on the condition of the existing asphalt and the bond quality. Reflective cracking typically initiates due to thermal contraction of the asphalt layer during cold periods, creating stress concentrations at existing crack tips. These stress concentrations are intensified by traffic loads, which further propagate cracks through the overlay.

Performance observations from test sections in US indicate that reflective cracking is influenced by the relative stiffness between the PCC overlay and the underlying HMA layer, in addition to the cumulative effects of repeated heavy traffic loading [18]. The stiffness ratio as shown in Eq.(3. 34), expressed as D_{PCC} / D_{HMA}, serves as an indicator of the likelihood of reflective crack formation.

$$D_{PCC/HMA} = \frac{E_{PCC} \times h_{PCC}^3}{E_{HMA} \times h_{HMA}^3} \left(\frac{1 - \mu_{HMA}^2}{1 - \mu_{PCC}^2} \right) \quad \textbf{(3. 34)}$$

When D_{PCC} / D_{HMA} is less than 1.0, the bonded concrete overlay is more susceptible to reflective cracking due to insufficient stiffness contrast with the asphalt layer. Such conditions reduce the overlay's ability to distribute stress effectively and increase the risk of crack propagation from the underlying pavement into the concrete layer.

In the BCOA-ME model developed by Pittsburgh University, the potential for reflective cracking is assessed after determining the required overlay thickness. The computed PCC thickness is used to evaluate the relative stiffness ratio D_{PCC} / D_{HMA}, with the risk of reflective cracking reported as a binary outcome—either "yes" or "no" based on whether the ratio falls below or above the threshold value of 1.0. This evaluation is diagnostic and does not influence the overlay thickness determined by the model. In practice, some state agencies accept the occurrence of limited reflective cracking, considering it non-critical to long-term performance and the achievement of design life. However, in cases where reflective cracking is a concern, several preventive strategies have been identified. These include thorough pre-overlay surface preparations such as milling, crack sealing, and targeted patching—to eliminate existing surface distress. Additionally, early-entry joint sawing aligned with known underlying cracks can help redirect and control crack propagation. Incorporating fiber reinforcement into the concrete mix is another effective strategy, as it enhances the material's post-cracking behavior by bridging cracks and reducing localized stress concentrations, thereby improving resistance to crack reflection.

3.9 Faulting Analysis

Faulting in BCOAs is primarily caused by traffic-induced pumping, which leads to progressive subgrade erosion and differential slab movement over time. To predict faulting behavior, the BCOA-ME model employs the Differential Energy (DE) concept, which estimates the relative elastic energy applied on the subgrade beneath the loaded and unloaded slab corners. This is expressed in Eq.(3. 35);

$$DE = E_L - E_{UL} = \frac{k\delta_L^2}{2} - \frac{k\delta_{UL}^2}{2} \quad \textbf{(3. 35)}$$

where k is the modulus of subgrade reaction, δ_L and δ_{UL} are the corner deflections under loaded and unloaded conditions, respectively. The difference in energy accumulation between the slab corners is used to quantify faulting potential.

The faulting model relies on an incremental prediction framework that incorporates both mechanistic calculations and data-driven methods. The model inputs include traffic, climate conditions, layer properties, and material characteristics of the erodible subgrade. These inputs feed into artificial neural networks, trained on finite element simulations and experimental performance data, to predict deflections, joint shear stress, and other critical responses. These are then used to calculate DE, the incremental differential energy at each timestep. The final faulting prediction is obtained through calibrated incremental faulting equations, supported by experimental data and standardized variability modeling. This hybrid approach enables BCOA-ME to estimate faulting progression under real-world traffic and environmental loading conditions, enhancing the reliability of overlay performance evaluations.

3.10 Wheel Wander

In BCOA model, particularly those with joint spacings exceeding 1.5m x 1.5 m (4 ft × 4 ft), the effect of wheel wander must be addressed to produce realistic fatigue life estimates. For overlays with a 2.0 m x 2.0 m (6 ft x 6 ft) joint spacing, FEM studies have shown that the critical stresses typically occur at the bottom of the PCC overlay within the wheelpath. However, due to lateral deviations in vehicle loading, stress concentrations are distributed over a wider area rather than consistently accumulating at a single point. To account for this, a fatigue adjustment factor is introduced in the BCOA-ME model. As described in the BCOA-ME Theory Manual, a wheel wander factor ($F_{wheelwander}$) is calculated as a function of the stress ratio (SR) using the empirical relationship, as seen in Eq.(3. 36)

$$F_{wheelwander} = 2.0405\ x\ SR^{-1.695} \quad \textbf{(3. 36)}$$

The adjustment enhances the predicted fatigue life by capturing the load distribution benefits of wheel wander, making it a crucial consideration in the mechanistic-empirical design of whitetopping systems.

CHAPTER 4

RESULTS AND ANALYSIS

With increasing traffic volumes, rising freight and passenger transport demands, and a growing number of vehicles per capita, the need for durable and cost-effective pavement technologies in Türkiye has become increasingly urgent. The country's highway network, currently dominated by asphalt pavements, is subject to frequent maintenance and major rehabilitation, particularly under heavy traffic loading. In this context, bonded concrete overlays on asphalt pavements, also referred to as thin whitetopping, represent a promising solution for extending pavement service life, improving ride quality, and enhancing long-term structural performance.

This study focused on applying the BCOA-ME design methodology, developed by the University of Pittsburgh, to ten provinces across Türkiye, each selected to reflect distinct climate conditions. Using a finite element-based approach, the BCOA-ME software was used to simulate overlay behavior and predict fatigue life under varying local conditions. Various design scenarios were examined, incorporating differences in traffic levels, subgrade stiffness (k-values), existing asphalt conditions, fiber reinforcement dosages, and slab configurations.

As shown in Table 3.1, key input parameters included a 20-year design life, C30/37 concrete class, varying traffic ESAL values (ranging from 5 million to 100 million), subgrade stiffness levels categorized as good (G: 350 pci / 95Mpa/m), moderate (M: 150 pci/ 41Mpa/m), and poor (P: 50 pci / 14Mpa/m), as well as three fiber content levels (0, 2.5, and 3.5 kg/m³). Joint spacing varied between small slabs (1×1 m) and large slabs (2×2 m) depending on structural adequacy and performance criteria.

In total, 1,440 design scenarios were evaluated using the BCOA-ME software. The recommended thicknesses for each of the ten provinces are presented in Table 4.1 through Table 4.10, providing a detailed and region-specific reference for bonded concrete overlay design. Thickness values marked with a “>” symbol indicate cases where a larger slab size is recommended due to limitations in fatigue performance or

reflective cracking risk. These results serve as a practical foundation for supporting the wider implementation of thin concrete overlays on existing asphalt pavements within Türkiye’s developing highway infrastructure.

Table 4.1 Recommended C30 Concrete Overlay Thickness for Afyonkarahisar

AFYONKARAHİSAR																																
HMA Fatique	ADEQUATE																															
Joint Spacing (m)	1.00X1.00 (SMALL SLAB)																															
ESAL Traffic	LOW									LOW-MODERATE									MODERATE-HIGH									HIGH					
Fiber Content (kg/m3)	0			2,5			3,5			0			2,5			3,5			0			2,5			3,5			0			2,5			3,5		
K value (Mpa/m)	G	M	P	G	M	P	G	M	P	G	M	P	G	M	P	G	M	P	G	M	P	G	M	P	G	M	P	G	M	P	G	M	P	G	M	P
Calculated PCC Overlay Thickness (mm)	136	136	135	120	119	118	116	115	114	>140	>140	>140	125	124	123	121	120	119	>140	>140	>140	126	126	125	122	122	121	>140	>140	>140	129	128	127	124	124	123
Joint Spacing (m)	2.00X2.00 (LARGE SLAB)																															
ESAL Traffic	LOW									LOW-MODERATE									MODERATE-HIGH									HIGH					
Fiber Content (kg/m3)	0			2,5			3,5			0			2,5			3,5			0			2,5			3,5			0			2,5			3,5		
K value (Mpa/m)	G	M	P	G	M	P	G	M	P	G	M	P	G	M	P	G	M	P	G	M	P	G	M	P	G	M	P	G	M	P	G	M	P	G	M	P
Calculated PCC Overlay Thickness (mm)	136	144	155	110	116	125	104	109	118	140	149	161	115	121	130	108	114	122	141	150	162	116	122	131	109	115	123	144	152	164	117	124	133	111	117	125
HMA Fatique	MARGINAL																															
Joint Spacing (m)	1.00X1.00 (SMALL SLAB)																															
ESAL Traffic	LOW									LOW-MODERATE									MODERATE-HIGH									HIGH					
Fiber Content (kg/m3)	0			2,5			3,5			0			2,5			3,5			0			2,5			3,5			0			2,5			3,5		
K value (Mpa/m)	G	M	P	G	M	P	G	M	P	G	M	P	G	M	P	G	M	P	G	M	P	G	M	P	G	M	P	G	M	P	G	M	P	G	M	P
Calculated PCC Overlay Thickness (mm)	137	137	136	121	121	120	117	117	115	>140	>140	>140	126	126	125	122	122	120	>140	>140	>140	128	127	126	123	123	122	>140	>140	>140	130	129	128	125	125	124
Joint Spacing (m)	2.00X2.00 (LARGE SLAB)																															
ESAL Traffic	LOW									LOW-MODERATE									MODERATE-HIGH									HIGH					
Fiber Content (kg/m3)	0			2,5			3,5			0			2,5			3,5			0			2,5			3,5			0			2,5			3,5		
K value (Mpa/m)	G	M	P	G	M	P	G	M	P	G	M	P	G	M	P	G	M	P	G	M	P	G	M	P	G	M	P	G	M	P	G	M	P	G	M	P
Calculated PCC Overlay Thickness (mm)	138	147	158	113	119	128	107	112	120	143	151	164	117	123	133	111	117	125	145	153	165	118	125	134	112	118	126	146	155	>165	120	126	136	114	119	129

Table 4.2 Recommended C30 Concrete Overlay Thickness for Erzurum

ERZURUM																																
HMA Fatique	ADEQUATE																															
Joint Spacing (m)	1.00X1.00 (SMALL SLAB)																															
ESAL Traffic	LOW									LOW-MODERATE									MODERATE-HIGH									HIGH					
Fiber Content (kg/m3)	0			2,5			3,5			0			2,5			3,5			0			2,5			3,5			0			2,5			3,5		
K value (Mpa/m)	G	M	P	G	M	P	G	M	P	G	M	P	G	M	P	G	M	P	G	M	P	G	M	P	G	M	P	G	M	P	G	M	P	G	M	P
Calculated PCC Overlay Thickness (mm)	137	137	136	120	120	119	116	116	114	>140	>140	>140	125	125	124	121	121	120	>140	>140	>140	127	126	125	123	122	121	>140	>140	>140	129	129	128	125	124	123
Joint Spacing (m)	2.00X2.00 (LARGE SLAB)																															
ESAL Traffic	LOW									LOW-MODERATE									MODERATE-HIGH									HIGH					
Fiber Content (kg/m3)	0			2,5			3,5			0			2,5			3,5			0			2,5			3,5			0			2,5			3,5		
K value (Mpa/m)	G	M	P	G	M	P	G	M	P	G	M	P	G	M	P	G	M	P	G	M	P	G	M	P	G	M	P	G	M	P	G	M	P	G	M	P
Calculated PCC Overlay Thickness (mm)	136	144	155	110	120	119	104	109	118	140	148	161	115	121	130	108	114	122	141	150	162	116	122	131	109	115	123	144	152	164	117	124	133	111	117	125
HMA Fatique	MARGINAL																															
Joint Spacing (m)	1.00X1.00 (SMALL SLAB)																															
ESAL Traffic	LOW									LOW-MODERATE									MODERATE-HIGH									HIGH					
Fiber Content (kg/m3)	0			2,5			3,5			0			2,5			3,5			0			2,5			3,5			0			2,5			3,5		
K value (Mpa/m)	G	M	P	G	M	P	G	M	P	G	M	P	G	M	P	G	M	P	G	M	P	G	M	P	G	M	P	G	M	P	G	M	P	G	M	P
Calculated PCC Overlay Thickness (mm)	138	138	137	122	121	120	117	117	116	>140	>140	>140	127	126	125	122	122	121	>140	>140	>140	128	128	127	124	123	122	>140	>140	>140	130	130	129	126	125	124
Joint Spacing (m)	2.00X2.00 (LARGE SLAB)																															
ESAL Traffic	LOW									LOW-MODERATE									MODERATE-HIGH									HIGH					
Fiber Content (kg/m3)	0			2,5			3,5			0			2,5			3,5			0			2,5			3,5			0			2,5			3,5		
K value (Mpa/m)	G	M	P	G	M	P	G	M	P	G	M	P	G	M	P	G	M	P	G	M	P	G	M	P	G	M	P	G	M	P	G	M	P	G	M	P
Calculated PCC Overlay Thickness (mm)	138	146	158	113	119	128	107	112	120	143	151	164	117	123	133	111	117	125	144	153	165	118	125	134	112	118	126	146	155	>165	120	126	136	114	119	129

Table 4.3 Recommended C30 Concrete Overlay Thickness for Eskişehir

ESKİŞEHİR																																
HMA Fatique	ADEQUATE																															
Joint Spacing (m)	1.00X1.00 (SMALL SLAB)																															
ESAL Traffic	LOW									LOW-MODERATE									MODERATE-HIGH									HIGH					
Fiber Content (kg/m3)	0			2,5			3,5			0			2,5			3,5			0			2,5			3,5			0			2,5			3,5		
K value (Mpa/m)	G	M	P	G	M	P	G	M	P	G	M	P	G	M	P	G	M	P	G	M	P	G	M	P	G	M	P	G	M	P	G	M	P	G	M	P
Calculated PCC Overlay Thickness (mm)	136	136	135	120	119	118	116	115	114	>140	>140	>140	125	125	123	121	120	119	>140	>140	>140	126	126	125	122	122	121	>140	>140	>140	129	128	127	124	124	123
Joint Spacing (m)	2.00X2.00 (LARGE SLAB)																															
ESAL Traffic	LOW									LOW-MODERATE									MODERATE-HIGH									HIGH					
Fiber Content (kg/m3)	0			2,5			3,5			0			2,5			3,5			0			2,5			3,5			0			2,5			3,5		
K value (Mpa/m)	G	M	P	G	M	P	G	M	P	G	M	P	G	M	P	G	M	P	G	M	P	G	M	P	G	M	P	G	M	P	G	M	P	G	M	P
Calculated PCC Overlay Thickness (mm)	136	144	155	110	116	125	104	110	118	140	149	161	115	121	130	108	114	122	142	150	162	116	122	131	109	115	124	144	152	164	117	124	133	111	117	126
HMA Fatique	MARGINAL																															
Joint Spacing (m)	1.00X1.00 (SMALL SLAB)																															
ESAL Traffic	LOW									LOW-MODERATE									MODERATE-HIGH									HIGH					
Fiber Content (kg/m3)	0			2,5			3,5			0			2,5			3,5			0			2,5			3,5			0			2,5			3,5		
K value (Mpa/m)	G	M	P	G	M	P	G	M	P	G	M	P	G	M	P	G	M	P	G	M	P	G	M	P	G	M	P	G	M	P	G	M	P	G	M	P
Calculated PCC Overlay Thickness (mm)	137	137	136	121	121	120	117	117	115	>140	>140	>140	126	126	125	122	122	120	>140	>140	>140	128	127	126	123	123	122	>140	>140	>140	130	130	128	125	125	124
Joint Spacing (m)	2.00X2.00 (LARGE SLAB)																															
ESAL Traffic	LOW									LOW-MODERATE									MODERATE-HIGH									HIGH					
Fiber Content (kg/m3)	0			2,5			3,5			0			2,5			3,5			0			2,5			3,5			0			2,5			3,5		
K value (Mpa/m)	G	M	P	G	M	P	G	M	P	G	M	P	G	M	P	G	M	P	G	M	P	G	M	P	G	M	P	G	M	P	G	M	P	G	M	P
Calculated PCC Overlay Thickness (mm)	139	147	158	113	119	128	107	113	121	143	152	164	117	124	133	111	117	125	145	153	>165	118	125	134	112	118	127	147	155	>165	120	126	136	114	120	129

Table 4.4 Recommended C30 Concrete Overlay Thickness for İstanbul

İSTANBUL																																
HMA Fatique	ADEQUATE																															
Joint Spacing (m)	1.00X1.00 (SMALL SLAB)																															
ESAL Traffic	LOW									LOW-MODERATE									MODERATE-HIGH									HIGH					
Fiber Content (kg/m3)	0			2,5			3,5			0			2,5			3,5			0			2,5			3,5			0			2,5			3,5		
K value (Mpa/m)	G	M	P	G	M	P	G	M	P	G	M	P	G	M	P	G	M	P	G	M	P	G	M	P	G	M	P	G	M	P	G	M	P	G	M	P
Calculated PCC Overlay Thickness (mm)	134	133	132	118	117	116	114	113	112	139	139	138	122	122	121	118	118	116	>140	>140	140	124	123	122	120	119	118	>140	>140	>140	126	126	124	122	121	120
Joint Spacing (m)	2.00X2.00 (LARGE SLAB)																															
ESAL Traffic	LOW									LOW-MODERATE									MODERATE-HIGH									HIGH					
Fiber Content (kg/m3)	0			2,5			3,5			0			2,5			3,5			0			2,5			3,5			0			2,5			3,5		
K value (Mpa/m)	G	M	P	G	M	P	G	M	P	G	M	P	G	M	P	G	M	P	G	M	P	G	M	P	G	M	P	G	M	P	G	M	P	G	M	P
Calculated PCC Overlay Thickness (mm)	137	145	157	111	117	126	104	110	118	139	147	159	113	119	128	106	112	120	143	151	164	116	122	132	109	116	124	145	153	>165	118	124	134	111	117	126
HMA Fatique	MARGINAL																															
Joint Spacing (m)	1.00X1.00 (SMALL SLAB)																															
ESAL Traffic	LOW									LOW-MODERATE									MODERATE-HIGH									HIGH					
Fiber Content (kg/m3)	0			2,5			3,5			0			2,5			3,5			0			2,5			3,5			0			2,5			3,5		
K value (Mpa/m)	G	M	P	G	M	P	G	M	P	G	M	P	G	M	P	G	M	P	G	M	P	G	M	P	G	M	P	G	M	P	G	M	P	G	M	P
Calculated PCC Overlay Thickness (mm)	135	135	134	119	118	117	115	114	113	>140	>140	139	123	123	122	119	119	118	>140	>140	>140	125	125	124	121	121	119	>140	>140	>140	127	127	126	123	123	121
Joint Spacing (m)	2.00X2.00 (LARGE SLAB)																															
ESAL Traffic	LOW									LOW-MODERATE									MODERATE-HIGH									HIGH					
Fiber Content (kg/m3)	0			2,5			3,5			0			2,5			3,5			0			2,5			3,5			0			2,5			3,5		
K value (Mpa/m)	G	M	P	G	M	P	G	M	P	G	M	P	G	M	P	G	M	P	G	M	P	G	M	P	G	M	P	G	M	P	G	M	P	G	M	P
Calculated PCC Overlay Thickness (mm)	139	148	160	114	120	129	107	113	121	142	150	162	116	122	131	109	115	123	146	154	>165	119	125	135	112	118	127	148	156	>165	121	127	137	114	120	129

Table 4.5 Recommended C30 Concrete Overlay Thickness for İzmir

İZMİR																																
HMA Fatique	ADEQUATE																															
Joint Spacing (m)	1.00X1.00 (SMALL SLAB)																															
ESAL Traffic	LOW									LOW-MODERATE									MODERATE-HIGH									HIGH					
Fiber Content (kg/m3)	0			2,5			3,5			0			2,5			3,5			0			2,5			3,5			0			2,5			3,5		
K value (Mpa/m)	G	M	P	G	M	P	G	M	P	G	M	P	G	M	P	G	M	P	G	M	P	G	M	P	G	M	P	G	M	P	G	M	P	G	M	P
Calculated PCC Overlay Thickness (mm)	134	134	133	118	117	116	114	113	112	139	139	138	123	122	121	119	118	117	>140	>140	140	124	124	123	120	120	118	>140	>140	>140	126	126	125	122	122	120
Joint Spacing (m)	2.00X2.00 (LARGE SLAB)																															
ESAL Traffic	LOW									LOW-MODERATE									MODERATE-HIGH									HIGH					
Fiber Content (kg/m3)	0			2,5			3,5			0			2,5			3,5			0			2,5			3,5			0			2,5			3,5		
K value (Mpa/m)	G	M	P	G	M	P	G	M	P	G	M	P	G	M	P	G	M	P	G	M	P	G	M	P	G	M	P	G	M	P	G	M	P	G	M	P
Calculated PCC Overlay Thickness (mm)	135	144	156	108	115	124	102	107	116	140	149	162	113	119	129	106	112	121	142	150	164	114	120	131	107	113	122	144	153	>165	116	122	133	109	115	124
HMA Fatique	MARGINAL																															
Joint Spacing (m)	1.00X1.00 (SMALL SLAB)																															
ESAL Traffic	LOW									LOW-MODERATE									MODERATE-HIGH									HIGH					
Fiber Content (kg/m3)	0			2,5			3,5			0			2,5			3,5			0			2,5			3,5			0			2,5			3,5		
K value (Mpa/m)	G	M	P	G	M	P	G	M	P	G	M	P	G	M	P	G	M	P	G	M	P	G	M	P	G	M	P	G	M	P	G	M	P	G	M	P
Calculated PCC Overlay Thickness (mm)	135	135	134	119	119	117	115	115	113	>140	>140	140	124	124	123	120	120	118	>140	>140	>140	125	125	124	121	121	120	>140	>140	>140	128	127	126	123	123	122
Joint Spacing (m)	2.00X2.00 (LARGE SLAB)																															
ESAL Traffic	LOW									LOW-MODERATE									MODERATE-HIGH									HIGH					
Fiber Content (kg/m3)	0			2,5			3,5			0			2,5			3,5			0			2,5			3,5			0			2,5			3,5		
K value (Mpa/m)	G	M	P	G	M	P	G	M	P	G	M	P	G	M	P	G	M	P	G	M	P	G	M	P	G	M	P	G	M	P	G	M	P	G	M	P
Calculated PCC Overlay Thickness (mm)	138	147	160	111	118	127	105	110	119	143	152	>165	116	122	132	109	115	124	145	154	>165	117	124	134	110	116	125	147	156	>165	119	125	136	112	118	128

Table 4.6 Recommended C30 Concrete Overlay Thickness for Kayseri

KAYSERİ																																		
HMA Fatique	ADEQUATE																																	
Joint Spacing (m)	1.00X1.00 (SMALL SLAB)																																	
ESAL Traffic	LOW									LOW-MODERATE									MODERATE-HIGH									HIGH							
Fiber Content (kg/m3)	0			2,5			3,5			0			2,5			3,5			0			2,5			3,5			0			2,5			3,5		
K value (Mpa/m)	G	M	P	G	M	P	G	M	P	G	M	P	G	M	P	G	M	P	G	M	P	G	M	P	G	M	P	G	M	P	G	M	P	G	M	P
Calculated PCC Overlay Thickness (mm)	138	138	137	121	120	119	117	116	115	>140	>140	>140	126	126	124	122	121	120	>140	>140	>140	128	127	126	123	123	121	>140	>140	>140	130	129	128	125	125	124
Joint Spacing (m)	2.00X2.00 (LARGE SLAB)																																	
ESAL Traffic	LOW									LOW-MODERATE									MODERATE-HIGH									HIGH							
Fiber Content (kg/m3)	0			2,5			3,5			0			2,5			3,5			0			2,5			3,5			0			2,5			3,5		
K value (Mpa/m)	G	M	P	G	M	P	G	M	P	G	M	P	G	M	P	G	M	P	G	M	P	G	M	P	G	M	P	G	M	P	G	M	P	G	M	P
Calculated PCC Overlay Thickness (mm)	136	144	156	111	117	126	105	110	118	141	149	161	115	121	131	109	115	123	142	151	163	116	122	132	110	116	124	144	153	165	118	124	134	112	117	126
HMA Fatique	MARGINAL																																	
Joint Spacing (m)	1.00X1.00 (SMALL SLAB)																																	
ESAL Traffic	LOW									LOW-MODERATE									MODERATE-HIGH									HIGH							
Fiber Content (kg/m3)	0			2,5			3,5			0			2,5			3,5			0			2,5			3,5			0			2,5			3,5		
K value (Mpa/m)	G	M	P	G	M	P	G	M	P	G	M	P	G	M	P	G	M	P	G	M	P	G	M	P	G	M	P	G	M	P	G	M	P	G	M	P
Calculated PCC Overlay Thickness (mm)	139	139	138	122	122	120	118	117	116	>140	>140	>140	127	127	126	123	122	121	>140	>140	>140	129	128	127	124	124	123	>140	>140	>140	131	131	130	126	126	125
Joint Spacing (m)	2.00X2.00 (LARGE SLAB)																																	
ESAL Traffic	LOW									LOW-MODERATE									MODERATE-HIGH									HIGH							
Fiber Content (kg/m3)	0			2,5			3,5			0			2,5			3,5			0			2,5			3,5			0			2,5			3,5		
K value (Mpa/m)	G	M	P	G	M	P	G	M	P	G	M	P	G	M	P	G	M	P	G	M	P	G	M	P	G	M	P	G	M	P	G	M	P	G	M	P
Calculated PCC Overlay Thickness (mm)	139	147	159	114	120	129	107	113	121	144	152	165	118	124	134	112	117	126	145	154	>165	119	125	135	113	118	127	147	155	>165	121	127	137	114	120	129

Table 4.7 Recommended C30 Concrete Overlay Thickness for Konya

KONYA																																
HMA Fatique	ADEQUATE																															
Joint Spacing (m)	1.00X1.00 (SMALL SLAB)																															
ESAL Traffic	LOW									LOW-MODERATE									MODERATE-HIGH									HIGH					
Fiber Content (kg/m3)	0			2,5			3,5			0			2,5			3,5			0			2,5			3,5			0			2,5			3,5		
K value (Mpa/m)	G	M	P	G	M	P	G	M	P	G	M	P	G	M	P	G	M	P	G	M	P	G	M	P	G	M	P	G	M	P	G	M	P	G	M	P
Calculated PCC Overlay Thickness (mm)	137	137	136	120	120	119	116	116	115	>140	>140	>140	126	125	124	121	121	120	>140	>140	>140	127	126	125	123	122	121	>140	>140	>140	129	129	128	125	124	123
Joint Spacing (m)	2.00X2.00 (LARGE SLAB)																															
ESAL Traffic	LOW									LOW-MODERATE									MODERATE-HIGH									HIGH					
Fiber Content (kg/m3)	0			2,5			3,5			0			2,5			3,5			0			2,5			3,5			0			2,5			3,5		
K value (Mpa/m)	G	M	P	G	M	P	G	M	P	G	M	P	G	M	P	G	M	P	G	M	P	G	M	P	G	M	P	G	M	P	G	M	P	G	M	P
Calculated PCC Overlay Thickness (mm)	137	145	156	111	117	126	105	110	118	141	149	162	115	121	131	109	115	123	142	151	163	116	123	132	110	116	124	144	153	>165	118	124	134	112	118	126
HMA Fatique	MARGINAL																															
Joint Spacing (m)	1.00X1.00 (SMALL SLAB)																															
ESAL Traffic	LOW									LOW-MODERATE									MODERATE-HIGH									HIGH					
Fiber Content (kg/m3)	0			2,5			3,5			0			2,5			3,5			0			2,5			3,5			0			2,5			3,5		
K value (Mpa/m)	G	M	P	G	M	P	G	M	P	G	M	P	G	M	P	G	M	P	G	M	P	G	M	P	G	M	P	G	M	P	G	M	P	G	M	P
Calculated PCC Overlay Thickness (mm)	137	137	136	120	120	119	116	116	115	>140	>140	140	126	125	124	121	121	120	>140	>140	>140	127	126	125	123	122	121	>140	>140	>140	129	129	128	125	124	123
Joint Spacing (m)	2.00X2.00 (LARGE SLAB)																															
ESAL Traffic	LOW									LOW-MODERATE									MODERATE-HIGH									HIGH					
Fiber Content (kg/m3)	0			2,5			3,5			0			2,5			3,5			0			2,5			3,5			0			2,5			3,5		
K value (Mpa/m)	G	M	P	G	M	P	G	M	P	G	M	P	G	M	P	G	M	P	G	M	P	G	M	P	G	M	P	G	M	P	G	M	P	G	M	P
Calculated PCC Overlay Thickness (mm)	137	145	156	111	117	126	105	110	118	141	149	162	115	121	131	109	115	123	142	151	163	116	123	132	110	116	124	144	153	>165	118	124	134	112	118	126

Table 4.8 Recommended C30 Concrete Overlay Thickness for Mersin

MERSİN																																
HMA Fatique	ADEQUATE																															
Joint Spacing (m)	1.00X1.00 (SMALL SLAB)																															
ESAL Traffic	LOW									LOW-MODERATE									MODERATE-HIGH									HIGH					
Fiber Content (kg/m3)	0			2,5			3,5			0			2,5			3,5			0			2,5			3,5			0			2,5			3,5		
K value (Mpa/m)	G	M	P	G	M	P	G	M	P	G	M	P	G	M	P	G	M	P	G	M	P	G	M	P	G	M	P	G	M	P	G	M	P	G	M	P
Calculated PCC Overlay Thickness (mm)	139	139	138	123	123	122	120	119	118	>140	>140	>140	129	128	127	124	124	123	>140	>140	>140	130	130	128	126	125	124	>140	>140	>140	132	132	130	128	127	126
Joint Spacing (m)	2.00X2.00 (LARGE SLAB)																															
ESAL Traffic	LOW									LOW-MODERATE									MODERATE-HIGH									HIGH					
Fiber Content (kg/m3)	0			2,5			3,5			0			2,5			3,5			0			2,5			3,5			0			2,5			3,5		
K value (Mpa/m)	G	M	P	G	M	P	G	M	P	G	M	P	G	M	P	G	M	P	G	M	P	G	M	P	G	M	P	G	M	P	G	M	P	G	M	P
Calculated PCC Overlay Thickness (mm)	142	151	165	114	120	131	107	113	122	147	157	>165	118	125	136	111	118	128	149	158	>165	119	127	138	112	119	129	151	161	>165	121	129	140	114	121	131
HMA Fatique	MARGINAL																															
Joint Spacing (m)	1.00X1.00 (SMALL SLAB)																															
ESAL Traffic	LOW									LOW-MODERATE									MODERATE-HIGH									HIGH					
Fiber Content (kg/m3)	0			2,5			3,5			0			2,5			3,5			0			2,5			3,5			0			2,5			3,5		
K value (Mpa/m)	G	M	P	G	M	P	G	M	P	G	M	P	G	M	P	G	M	P	G	M	P	G	M	P	G	M	P	G	M	P	G	M	P	G	M	P
Calculated PCC Overlay Thickness (mm)	>140	>140	139	124	124	123	121	120	119	>140	>140	>140	130	129	128	125	125	124	>140	>140	>140	131	130	129	127	126	125	>140	>140	>140	133	132	131	129	128	127
Joint Spacing (m)	2.00X2.00 (LARGE SLAB)																															
ESAL Traffic	LOW									LOW-MODERATE									MODERATE-HIGH									HIGH					
Fiber Content (kg/m3)	0			2,5			3,5			0			2,5			3,5			0			2,5			3,5			0			2,5			3,5		
K value (Mpa/m)	G	M	P	G	M	P	G	M	P	G	M	P	G	M	P	G	M	P	G	M	P	G	M	P	G	M	P	G	M	P	G	M	P	G	M	P
Calculated PCC Overlay Thickness (mm)	145	154	>165	117	123	134	109	116	125	150	160	>165	121	128	139	114	120	131	152	161	>165	122	130	141	115	122	132	154	163	>165	124	132	143	117	124	134

Table 4.9 Recommended C30 Concrete Overlay Thickness for Rize

RİZE																																
HMA Fatique	ADEQUATE																															
Joint Spacing (m)	1.00X1.00 (SMALL SLAB)																															
ESAL Traffic	LOW									LOW-MODERATE									MODERATE-HIGH									HIGH					
Fiber Content (kg/m3)	0			2,5			3,5			0			2,5			3,5			0			2,5			3,5			0			2,5			3,5		
K value (Mpa/m)	G	M	P	G	M	P	G	M	P	G	M	P	G	M	P	G	M	P	G	M	P	G	M	P	G	M	P	G	M	P	G	M	P	G	M	P
Calculated PCC Overlay Thickness (mm)	133	133	132	117	117	115	113	113	111	139	139	138	122	122	121	118	118	116	>140	>140	139	123	123	122	119	119	118	>140	>140	>140	126	125	124	121	121	120
Joint Spacing (m)	2.00X2.00 (LARGE SLAB)																															
ESAL Traffic	LOW									LOW-MODERATE									MODERATE-HIGH									HIGH					
Fiber Content (kg/m3)	0			2,5			3,5			0			2,5			3,5			0			2,5			3,5			0			2,5			3,5		
K value (Mpa/m)	G	M	P	G	M	P	G	M	P	G	M	P	G	M	P	G	M	P	G	M	P	G	M	P	G	M	P	G	M	P	G	M	P	G	M	P
Calculated PCC Overlay Thickness (mm)	137	145	157	111	117	126	105	110	118	141	150	162	115	121	131	108	114	123	143	151	164	116	123	132	110	116	124	145	153	>165	118	124	134	111	117	126
HMA Fatique	MARGINAL																															
Joint Spacing (m)	1.00X1.00 (SMALL SLAB)																															
ESAL Traffic	LOW									LOW-MODERATE									MODERATE-HIGH									HIGH					
Fiber Content (kg/m3)	0			2,5			3,5			0			2,5			3,5			0			2,5			3,5			0			2,5			3,5		
K value (Mpa/m)	G	M	P	G	M	P	G	M	P	G	M	P	G	M	P	G	M	P	G	M	P	G	M	P	G	M	P	G	M	P	G	M	P	G	M	P
Calculated PCC Overlay Thickness (mm)	134	134	133	118	118	117	115	114	113	>140	>140	139	123	123	122	119	119	118	>140	>140	>140	125	124	123	121	120	119	>140	>140	>140	127	126	125	123	122	121
Joint Spacing (m)	2.00X2.00 (LARGE SLAB)																															
ESAL Traffic	LOW									LOW-MODERATE									MODERATE-HIGH									HIGH					
Fiber Content (kg/m3)	0			2,5			3,5			0			2,5			3,5			0			2,5			3,5			0			2,5			3,5		
K value (Mpa/m)	G	M	P	G	M	P	G	M	P	G	M	P	G	M	P	G	M	P	G	M	P	G	M	P	G	M	P	G	M	P	G	M	P	G	M	P
Calculated PCC Overlay Thickness (mm)	140	148	160	114	120	129	107	113	121	144	153	>165	118	124	134	111	117	126	146	154	>165	119	125	135	112	118	128	148	156	>165	121	127	137	114	120	129

Table 4.10 Recommended C30 Concrete Overlay Thickness for Şanlıurfa

ŞANLIURFA																																
HMA Fatique	ADEQUATE																															
Joint Spacing (m)	1.00X1.00 (SMALL SLAB)																															
ESAL Traffic	LOW									LOW-MODERATE									MODERATE-HIGH									HIGH					
Fiber Content (kg/m3)	0			2,5			3,5			0			2,5			3,5			0			2,5			3,5			0			2,5			3,5		
K value (Mpa/m)	G	M	P	G	M	P	G	M	P	G	M	P	G	M	P	G	M	P	G	M	P	G	M	P	G	M	P	G	M	P	G	M	P	G	M	P
Calculated PCC Overlay Thickness (mm)	>140	>140	139	124	124	122	120	120	118	>140	>140	>140	129	129	128	125	124	123	>140	>140	>140	131	130	129	126	126	125	>140	>140	>140	131	130	129	126	126	125
Joint Spacing (m)	2.00X2.00 (LARGE SLAB)																															
ESAL Traffic	LOW									LOW-MODERATE									MODERATE-HIGH									HIGH					
Fiber Content (kg/m3)	0			2,5			3,5			0			2,5			3,5			0			2,5			3,5			0			2,5			3,5		
K value (Mpa/m)	G	M	P	G	M	P	G	M	P	G	M	P	G	M	P	G	M	P	G	M	P	G	M	P	G	M	P	G	M	P	G	M	P	G	M	P
Calculated PCC Overlay Thickness (mm)	142	151	164	113	120	130	106	112	122	147	156	>165	118	125	136	111	117	127	148	158	>165	119	126	137	112	118	129	148	158	>165	119	126	137	112	118	129
HMA Fatique	MARGINAL																															
Joint Spacing (m)	1.00X1.00 (SMALL SLAB)																															
ESAL Traffic	LOW									LOW-MODERATE									MODERATE-HIGH									HIGH					
Fiber Content (kg/m3)	0			2,5			3,5			0			2,5			3,5			0			2,5			3,5			0			2,5			3,5		
K value (Mpa/m)	G	M	P	G	M	P	G	M	P	G	M	P	G	M	P	G	M	P	G	M	P	G	M	P	G	M	P	G	M	P	G	M	P	G	M	P
Calculated PCC Overlay Thickness (mm)	>140	>140	>140	125	125	123	121	121	119	>140	>140	>140	130	130	129	126	125	124	>140	>140	>140	132	131	130	127	127	126	>140	>140	>140	132	131	130	127	127	126
Joint Spacing (m)	2.00X2.00 (LARGE SLAB)																															
ESAL Traffic	LOW									LOW-MODERATE									MODERATE-HIGH									HIGH					
Fiber Content (kg/m3)	0			2,5			3,5			0			2,5			3,5			0			2,5			3,5			0			2,5			3,5		
K value (Mpa/m)	G	M	P	G	M	P	G	M	P	G	M	P	G	M	P	G	M	P	G	M	P	G	M	P	G	M	P	G	M	P	G	M	P	G	M	P
Calculated PCC Overlay Thickness (mm)	145	154	>165	116	123	133	109	115	125	150	159	>165	121	128	139	114	120	130	151	161	>165	122	129	140	115	121	132	151	161	>165	122	129	140	115	121	132

4.1 Fiber Effect

Synthetic fibers are not intended to replace primary reinforcement in concrete due to their relatively limited contribution to structural strength. However, since the benefits of traditional reinforcement become effective only after concrete hardens, synthetic fibers play a valuable complementary role—particularly during the plastic phase. While the concrete is still fresh, fibers help control early-age cracking and improve overall durability. Their ability to bridge microcracks makes them especially beneficial in thin concrete overlays, where plastic shrinkage and early cracking are common concerns.

The use of fibers in bonded concrete overlays has seen steady growth, primarily because of their dual role in mitigating shrinkage cracking and improving post-cracking flexural behavior. At higher dosages, synthetic macrofibers enhance load distribution and fatigue resistance, often making it possible to construct overlays without dowel or tie bars. Practical applications in the United States suggest that structural benefits begin to manifest at fiber dosages above 4.0–4.5 lb/yd³ (approximately 2.5 kg/m³). According to Bordelon and Roesler, (2012) a minimum R_{150} value of 20% corresponding to residual strengths between 0.7 MPa and 1.0 MPa (100–150 psi) is recommended for fiber-reinforced overlays to achieve meaningful structural contribution [27].

In this study, fiber reinforcement demonstrated a significant impact on the thickness design of bonded concrete overlays. As presented in Tables 4.1 through 4.10, the reduction values were derived based on the relative thickness ratio between the unreinforced case (0% fiber dosage) and the fiber-reinforced alternatives. Specifically, values were computed using the ratio of unreinforced thickness to fiber-reinforced thickness (e.g., 165 mm / 124 mm = 1.33), and interpreted as indicative of relative structural efficiency.

Although this method highlights the proportional decrease in required thickness, it should be noted that these are not direct percentage reductions based on the absolute difference. For instance, a relative thickness ratio of 1.33—calculated as unreinforced thickness divided by fiber-reinforced thickness—corresponds to a true reduction of

approximately 25%. All thickness reduction values reported in this study are based on the relative thickness ratio between fiber-reinforced and unreinforced overlays unless stated otherwise. The following values represent observed relative reductions derived from this ratio-based approach:

- Afyonkarahisar – maximum 32%, average 21%
- Erzurum – maximum 32%, average 21%
- Eskişehir – maximum 32%, average 21%
- Istanbul – maximum 33%, average 22%
- Izmir – maximum 35%, average 23%
- Kayseri – maximum 32%, average 21%
- Konya – maximum 32%, average 22%
- Mersin – maximum 35%, average 21%
- Rize – maximum 32%, average 22%
- Şanlıurfa – maximum 35%, average 21%

When all provinces and scenarios are considered collectively, the use of 3.5 kg/m³ synthetic fiber results in a maximum relative thickness reduction of approximately 35%, with an average reduction of around 24%. In comparison, the 2.5 kg/m³ fiber dosage provides a slightly lower average reduction of approximately 19%. In colder regions, such as those with severe winter conditions, the maximum observed reductions remained closer to 30% [45]. These findings emphasize the cost-effectiveness and performance advantages of fiber-reinforced thin concrete overlays, particularly in the context of Türkiye's heavily trafficked and maintenance-intensive highway infrastructure.

Since it is not feasible to generate graphical comparisons for all design scenarios, a representative reference case was selected to present the fiber effect visually. A reference scenario was established, characterized by moderate-to-low ESAL levels, moderate subgrade stiffness, adequate existing HMA condition, and a small joint spacing configuration. This baseline condition provides a balanced and practical framework for assessing the effects of fiber content, joint spacing, subgrade support, and traffic loading across various climatic regions. Based on this specific scenario, the change in overlay thickness with increasing fiber dosage is illustrated in Figure 4. 1.

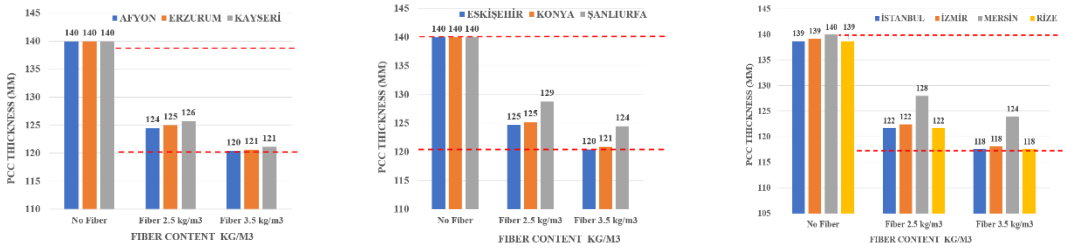

Figure 4. 1 PCC Thickness vs Fiber Amount Graphics of ten provinces in case of fiber quantity increasing from zero to 3.5 kg/m3 (for the case of ESAL low-moderate, fatigue-Adequate, subgrade k value-moderate, joint spacing 1x1 m).

Additionally, the difference in relative thickness reduction between 2.5 kg/m³ and 3.5 kg/m³ fiber dosage is generally around 5%. In the specific reference case—where all design variables were set to moderate levels, this reduction ranged between 3% and 4%, as shown in Figure 4.2. This trend suggests diminishing returns at higher fiber contents, highlighting the importance of optimizing fiber dosage in each design scenario to achieve a balance between structural performance improvements and material cost efficiency.

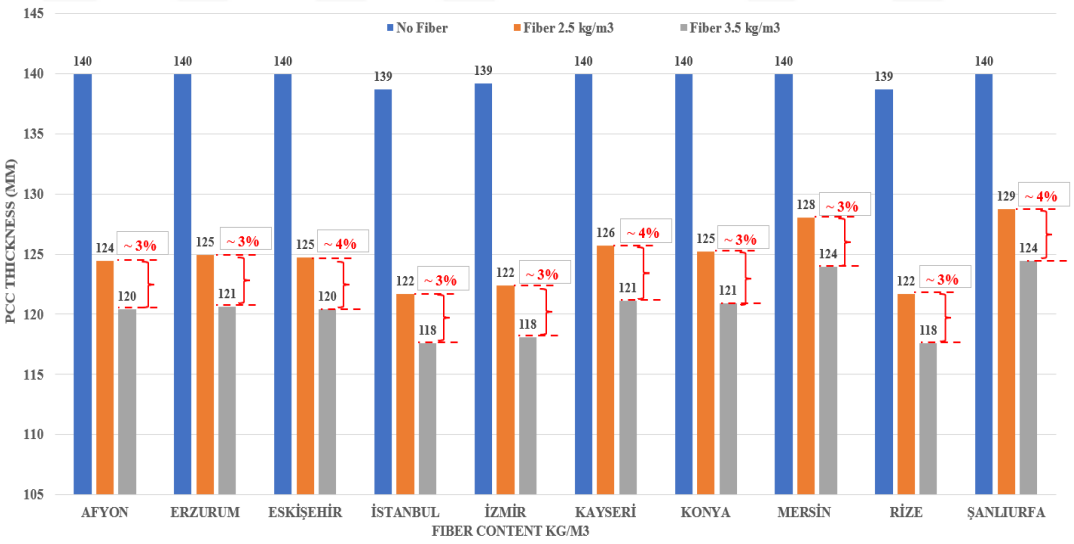

Figure 4. 2 PCC Thickness vs Fiber Amount Graphic of ten provinces (for the case of ESAL low-moderate, fatigue-Adequate, subgrade k value-moderate, joint spacing 1x1 m).

The variation in thickness reduction provided by fiber reinforcement across different scenarios can be attributed to the combined effects of climate conditions, subgrade stiffness, traffic loading, joint spacing, and the structural condition of the existing asphalt layer. In moderate-stress environments, where the baseline stress ratio is near critical fatigue thresholds, fiber reinforcement significantly enhances performance by increasing effective flexural strength and extending fatigue life—resulting in notable thickness reductions. In very high-stress conditions (e.g., weak subgrade, large slab sizes, or harsh climates), however, the contribution of fibers may be insufficient to reduce the stress ratio below acceptable limits, thereby limiting their impact on thickness. Conversely, in low-stress scenarios, where fatigue criteria are already satisfied, the benefit of fiber addition becomes less pronounced. As a result, the effectiveness of fibers in reducing overlay thickness is highly dependent on the interaction of design inputs and baseline stress levels. However, in this study, under high-stress conditions—such as large slab configurations or weak subgrade soils—fibers exhibit a more significant structural contribution, leading to pavement thickness reductions of around 20-30% based on the relative thickness ratio as shown in Figure 4. 3.

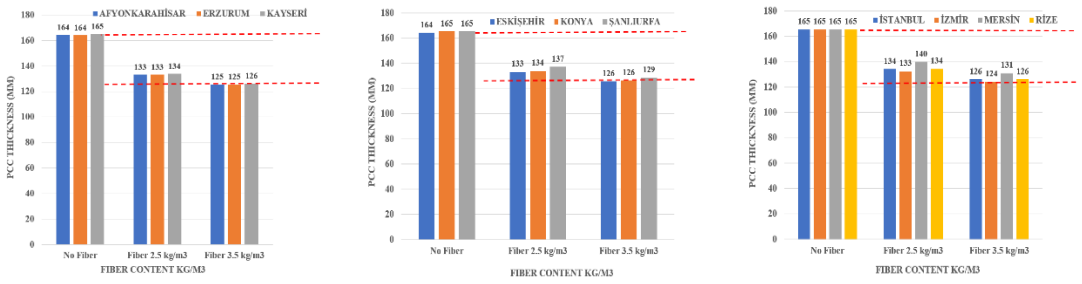

Figure 4. 3 PCC Thickness vs Fiber Amount Graphic of ten provinces (for the case of ESAL-high, fatigue-Adequate, subgrade k value-poor, joint spacing 2x2 m).

4.2 Climate Effect

The climatic conditions of a region play a vital role in the structural design of bonded concrete overlays by influencing the thermal behavior of the pavement system. In BCOA designs, the most critical climate-related factor is the ΔT caused by daily/seasonally surface heating and cooling. This gradient, often represented by the

EELTG, directly affects the development of thermally induced stresses such as slab curling and tensile cracking at the base of the overlay. These thermal stresses increase the total design stress (σ), which in turn affects the stress ratio (SR) and required overlay thickness to meet fatigue performance thresholds. Regions with severe daily temperature fluctuations or long sunshine duration typically exhibit higher ΔT values, demanding thicker overlays even under moderate traffic or subgrade conditions.

While cold regions such as Erzurum and Kayseri are typically expected to require thicker overlays due to freeze–thaw cycles and temperature-induced contraction, the findings of this study reveal that certain hot and high-sunshine regions—such as Şanlıurfa and Mersin—also exhibit elevated thickness demands under specific conditions. This is particularly evident in large slab configurations (Figure 4. 4) compared to small slab cases (Figure 4. 5), where other parameters were held constant for direct comparison. This can be attributed to their high annual sunshine percentages (S_{ave}) and intense solar radiation, which increase pavement surface temperatures during the day and generate significant thermal gradients. These findings highlight the importance of considering climate-induced stresses—not only cold-related—but also solar-driven thermal gradients in pavement design, especially in arid and semi-arid regions of Türkiye.

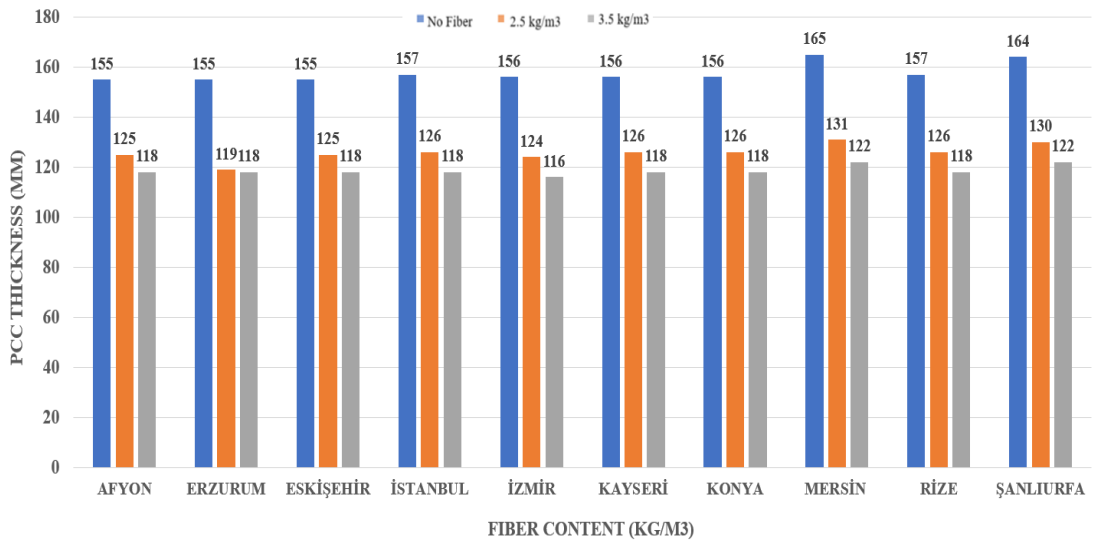

Figure 4. 4 PCC Thickness vs Fiber Amount Graphic of ten provinces (for the case of ESAL-low, fatigue-Adequate, subgrade k value-poor, joint spacing 2x2 m).

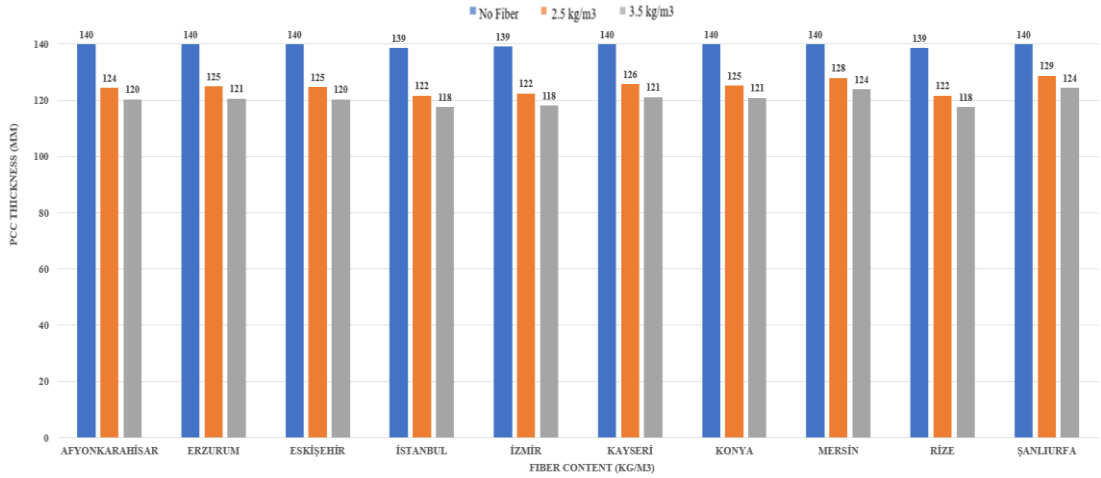

Figure 4. 5 PCC Thickness vs Fiber Amount Graphic of ten provinces (for the case of ESAL low-moderate, fatigue-Adequate, subgrade k value-moderate, joint spacing 1x1 m).

4.3 Traffic Volume Effect

As expected, increasing traffic volumes—represented by ESAL valued to a corresponding increase in BCOA thickness. The thickness design trend was upward across low, moderate, and high ESAL categories, as illustrated in Figure 4. 6 for a representative scenario. However, the observed increase in overlay thickness was relatively modest, generally ranging between 5% and 8% across traffic levels. Compared to traditional concrete pavement design, where traffic loading significantly influences slab thickness, the impact of ESAL in BCOA design appears to be more constrained. This can be attributed to several factors inherent in the BCOA-ME framework: overlay thickness recommendations are limited to practical ranges (typically under 15 cm) due to constructability and cost-effectiveness; the use of small joint spacing (e.g., 1.0 × 1.0 m) helps distribute loads more evenly; and in ultra-thin whitetopping applications, a single axle load rarely affects an entire slab. These factors collectively moderate the influence of traffic loading, resulting in more efficient and thinner designs even under relatively high ESAL conditions.

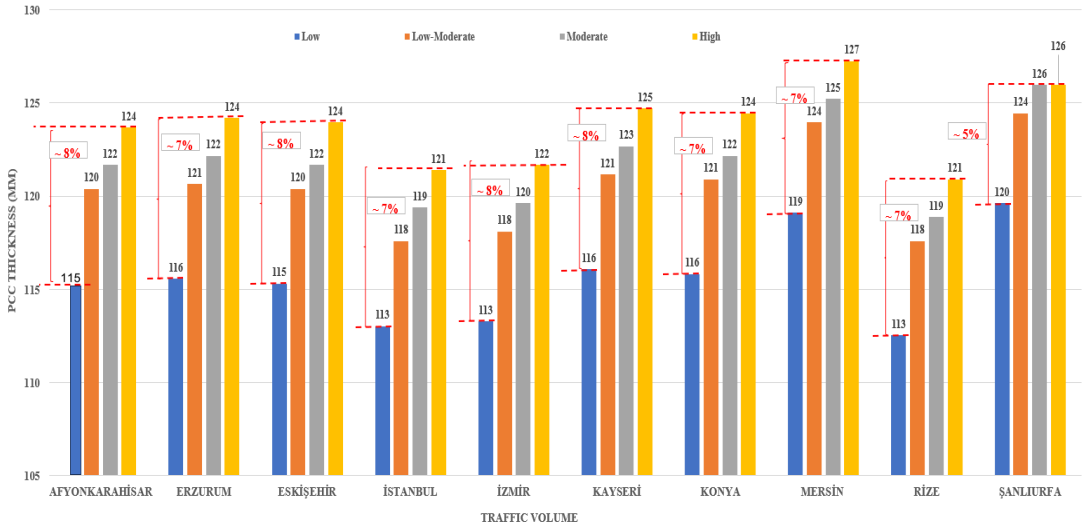

Figure 4. 6 PCC Thickness vs Traffic Volume Graphics of ten provinces (for the case of fatigue-Adequate, subgrade k value-moderate, fiber content-max and joint spacing is 1x1 m).

4.4 Joint Spacing Effect

The influence of joint spacing on overlay thickness is clearly demonstrated when comparing small and large slab configurations, as illustrated in Figure 4. 7. In fiber-free cases, smaller slabs (1.0 × 1.0 m) consistently result in thinner overlay designs due to their shorter bending spans and reduced flexural stress concentrations. Across different scenarios, joint spacing reduction led to a relative thickness decrease of approximately 13–19%. However, this expected trend was not consistently observed when fiber reinforcement was introduced. As seen in Tables 4.1 to 4.10 and Figure 4. 7, fiber-reinforced overlays with small slabs sometimes resulted in comparable or even slightly greater thickness than large-slab configurations (2.0 × 2.0 m).

This variation arises from the internal structure of the BCOA-ME software. The model classifies joint spacing into three categories: less than 4.5 ft-1.5m (small slabs), between 4.5 ft -1.5m and 6.5 ft-2.0m (medium), and full-width slabs. Importantly, wheel wander effects—which account for lateral vehicle movement—are only considered for slabs greater than 4.5 ft-1.5m. In such cases, the load is more evenly distributed across the slab, reducing the frequency of critical stress applications and increasing effective fatigue life. This lateral load distribution can offset the expected

stress advantage of small slabs in fiber-reinforced conditions, leading to unexpected thickness outcomes.

These findings also suggest that fiber addition may provide design flexibility in joint spacing, allowing the use of wider slabs without sacrificing performance. While small, fiber-free slabs may offer thickness benefits, fiber-reinforced overlays with larger joint spacing and the same thickness can achieve similar, potentially simplifying construction. However, further experimental research is needed to confirm the impact of fibers on load transfer efficiency (LTE) and to validate the design assumptions embedded within the BCOA-ME model.

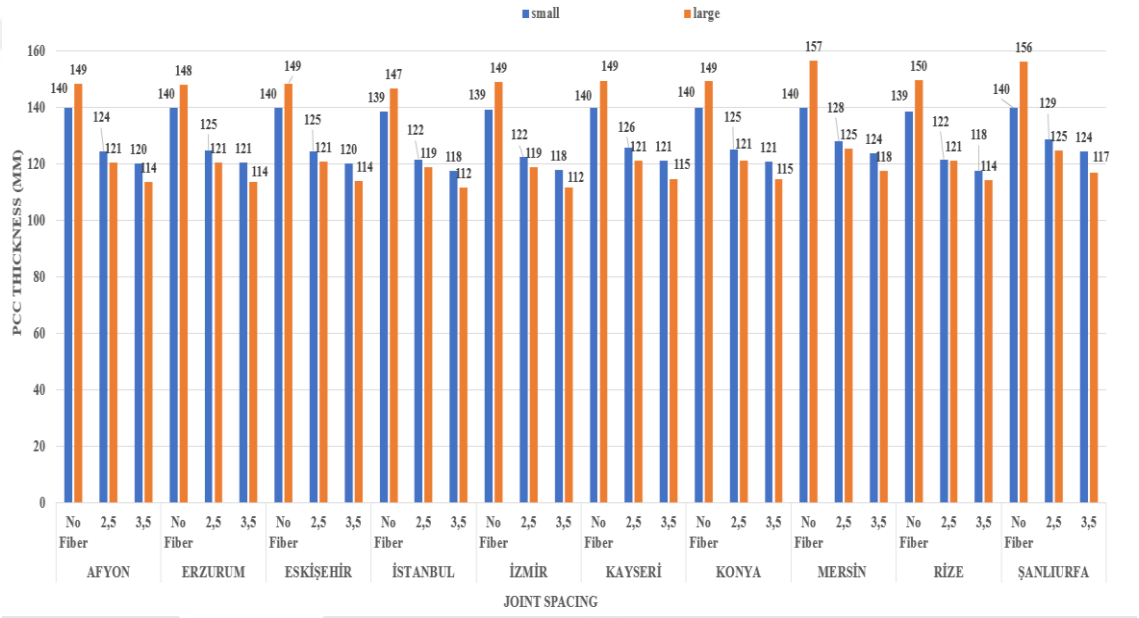

Figure 4. 7 PCC Thickness vs Fiber Content-Cities Graphic of ten provinces in case of small and large slab (for the case of ESAL low-moderate, fatigue-Adequate, subgrade k value-moderate).

4.4.1 Subgrade Effect

The effect of subgrade stiffness (k-value) on bonded overlay thickness design was found to vary significantly with slab size, as illustrated in Figure 4. 8 and Figure 4. 9. In configurations with small slab sizes (1.0 × 1.0 m), increasing the subgrade modulus from poor (50 pci) to good (350 pci) resulted in negligible changes in overlay thickness. This behavior can be attributed to the inherently stiff structural action of

small slabs, which distribute loads over a limited span and are thus less dependent on the elastic support provided by the subgrade. In other words, the shorter bending length reduces deflection sensitivity to subgrade variations, meaning that even in weak soil conditions, the induced stress levels may remain within acceptable limits for fatigue performance.

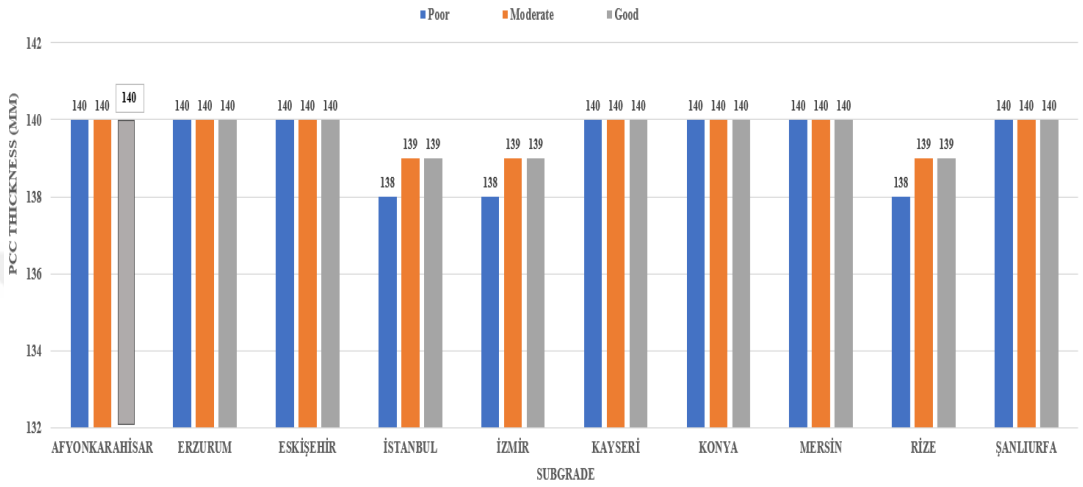

Figure 4. 8 PCC Thickness vs Subgrade Graphic of ten provinces (for the case of ESAL low-moderate, fatigue-Adequate, joint spacing 1x1 m and no fiber)

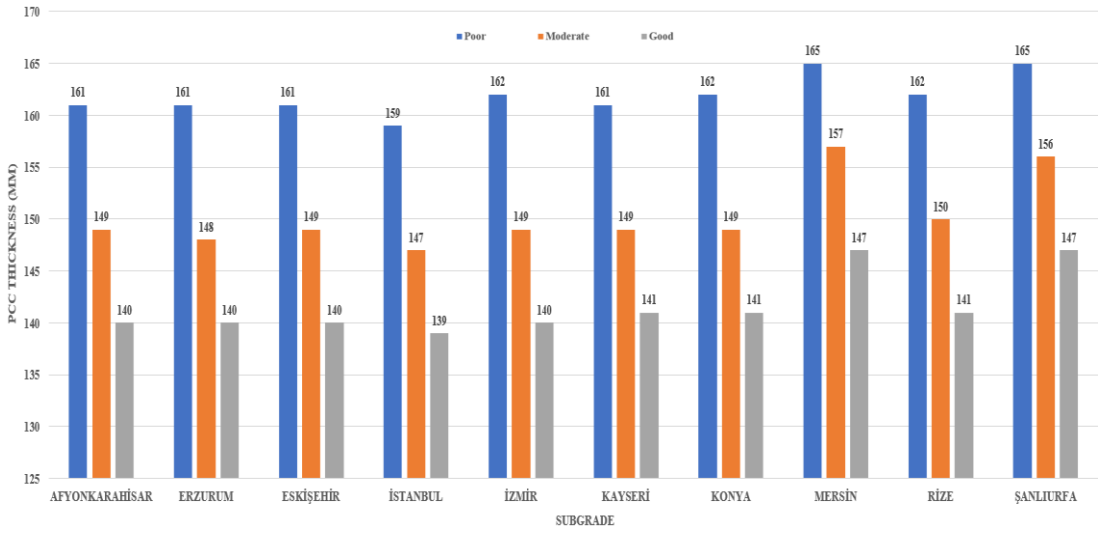

Figure 4. 9 PCC Thickness vs Subgrade Graphic of ten provinces (for the case of ESAL low-moderate, fatigue-Adequate, joint spacing 2x2 m and no fiber)

In contrast, large slab configurations (2.0 × 2.0 m) exhibit much greater sensitivity to subgrade support conditions. As the slab size increases, the effective bending span also increases, making the structural response of the overlay more dependent on the stiffness of the underlying materials. In these scenarios, poor subgrade support can lead to higher flexural stress at the bottom of the slab due to greater deflection under loading. However, as the subgrade condition improves—from poor to moderate or good—the reduction in vertical deformation translates into lower tensile stress levels in the overlay. As shown in Figure 4. 10, thickness reductions of up to 15% were observed between poor and good subgrade conditions in large slab configurations.

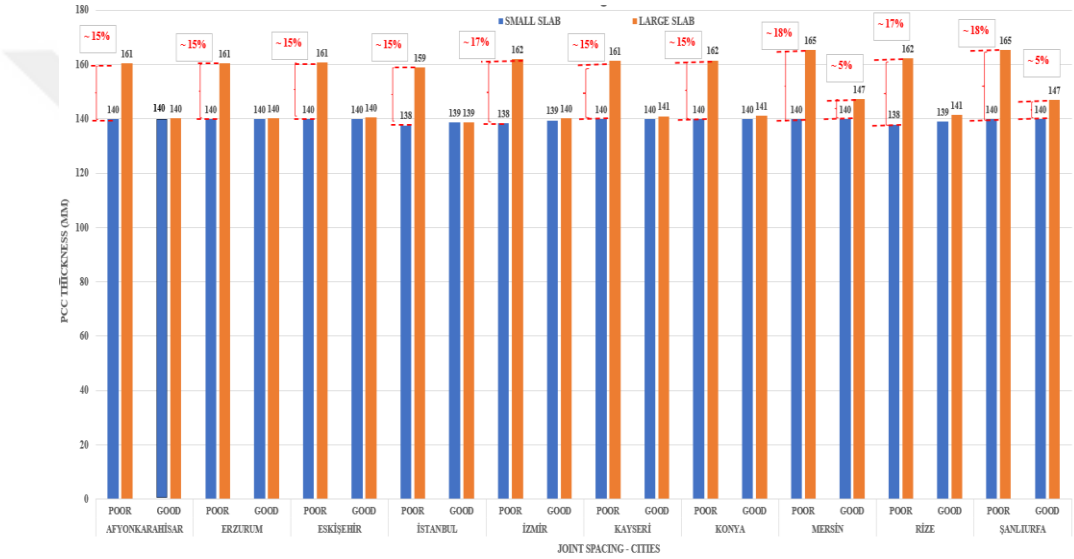

Figure 4. 10 PCC Thickness vs Joint Spacing Graphics of ten provinces (k value from poor to good while thickness variation for small and large slab of ten provinces for the case of traffic-low moderate, fatigue-Adequate, k value-poor to good, no fiber)

4.5 Structural Condition of the Asphalt layer

The condition of the existing asphalt (HMA) layer plays a key role in bonded concrete overlay design by influencing the structural support provided to the overlay. Within the BCOA-ME framework, the HMA condition is classified as either adequate or marginal, depending on the extent of fatigue cracking in the existing pavement. Adequate layers (with less than 8% fatigue cracking) are assigned a damage factor of

0.3, while marginal layers (with 8–20% cracking) are assigned a factor of 0.4, resulting in modulus reductions of 5% and 12.5%, respectively.

In this study, the impact of the existing HMA layer on overlay thickness was evaluated by comparing design outcomes under both adequate and marginal structural scenarios. As illustrated in Figure 4. 11, changing the HMA condition from adequate (fatigue cracking < 8%) to marginal (fatigue cracking between 8% and 20%) resulted in only a minor increase in overlay thickness, with observed differences not exceeding 5% in most cases.

The limited influence of the HMA condition can be primarily attributed to the high stiffness of the concrete overlay, which governs the structural behavior of the composite system. Since the overlay layer dominates the load distribution and stress response, moderate degradation in the underlying asphalt has only a secondary effect. Additionally, the BCOA-ME design approach applies HMA degradation indirectly by adjusting the asphalt modulus through a damage factor. This method of adjustment has less impact on the design thickness compared to other variables such as subgrade stiffness or fiber reinforcement, which more directly affect the critical stress and fatigue performance.

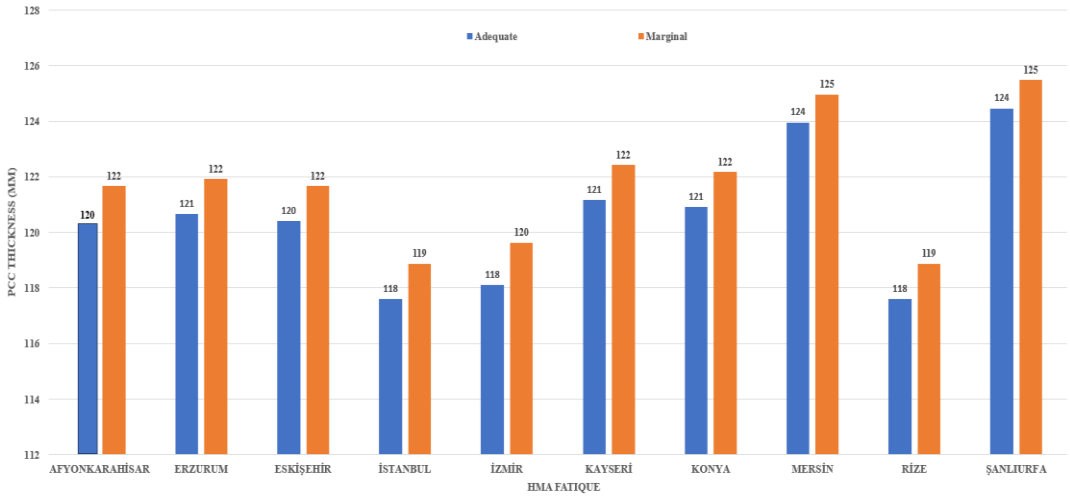

Figure 4. 11 PCC Thickness vs Fatigue Graphics of ten provinces (for the case of ESAL low-moderate, fatigue-Adequate, k value-moderate, joint spacing 1x1 m and Fiber Content 3.5 kg/m3)

CHAPTER 5

TOOL DEVELOPMENT

In this chapter, a user-friendly tool is introduced, developed using the results obtained from the BCOA-ME program created by the University of Pittsburgh. The purpose of the tool is to facilitate the preliminary design of bonded concrete overlay thicknesses for ten representative cities in Türkiye. Users can input key variables such as traffic volume, subgrade stiffness, condition of the existing asphalt pavement, fiber content, and joint spacing. Based on these selections, the tool provides recommended overlay thicknesses adapted from a database of 1,440 scenarios evaluated in this study.

This tool is particularly valuable for contractors, designers, and public agencies involved in early-stage planning and bidding, where project-specific field data (such as on-site traffic counts or fatigue mapping) may not yet be available. By using default or typical values, it helps support quick and informed decision-making during the proposal or concept design phase.

The current version represents the initial stage of development. In future phases, the tool aims to be fully adapted to Türkiye's national conditions by integrating local climate data, refining calibration factors, and incorporating validated material parameters through laboratory studies and field observations. Long-term performance monitoring of overlays will also contribute to improving the tool's accuracy and reliability. Access to the tool is available via the QR code and hyperlink provided below.



http://anabasist.xyz/

CHAPTER 6

CONCLUSION AND RECOMMENDATIONS

6.1 Conclusion

Türkiye's growing freight and passenger transportation demand—largely met through its asphalt-dominated highway network—has increased the need for cost-effective and durable pavement rehabilitation strategies. This study evaluated the performance of bonded concrete overlays on asphalt (BCOA) using a mechanistic-empirical framework (BCOA-ME) developed by the University of Pittsburgh. A total of 1,440 simulations were performed using the BCOA-ME software developed by the University of Pittsburgh, which utilizes a finite element-based, mechanistic-empirical approach to predict overlay performance under varying field conditions.

The design scenarios incorporated several key variables. The concrete used was C30/37, a standard mix class for pavement applications. A 20-year design life was assumed, along with a 15% slab replacement rate to reflect potential localized failures. A reliability level of 85% was adopted to account for variability in field conditions and performance prediction. Traffic loading was categorized into four levels: low (~5 million ESALs), low-moderate (~30 million), moderate-high (~50 million), and high (~100 million). The modulus of subgrade reaction (k-value) was classified into three levels: poor (50 pci / 14 MPa/m), moderate (150 pci / 41 MPa/m), and good (350 pci / 95 MPa/m). To assess the impact of fiber reinforcement, fiber contents were considered at 0 kg/m³ (unreinforced), 2.5 kg/m³ (~0.25%), and 3.5 kg/m³ (~0.5%). Two structural conditions of the existing Hot Mix Asphalt (HMA) layer—adequate and marginal—were also considered to reflect varying degrees of fatigue damage in the asphalt base. Finally, two joint spacing configurations were evaluated: small slabs (1×1 m) and large slabs (2×2 m). The study aimed to deliver regionally adapted thickness design recommendations and offer a user-friendly digital tool to support engineers and agencies in practical overlay applications.

The following key conclusions were drawn:

- Fiber reinforcement demonstrated a notable impact on overlay thickness design. Based on the relative thickness ratio, the incorporation of 3.5 kg/m³ synthetic fiber yielded a maximum reduction of approximately 35%, with an average reduction of around 24%. In comparison, the 2.5 kg/m³ dosage resulted in an average reduction of about 19%. The relatively modest difference in performance between the two dosages highlights the importance of optimizing fiber content according to specific project requirements to balance structural benefits and cost-efficiency.
- Fiber reinforcement was more effective in large slabs. Large slabs (2×2 m) benefited from up to 10% greater thickness reduction than small slabs. This implies a stronger structural role for fibers when bending spans are longer, although more research is needed in this area.
- Cities with high solar exposure and sunshine percentages (e.g., Şanlıurfa, Mersin) showed elevated thickness demands due to thermal gradients. This pattern occurred despite expectations that cold cities like Erzurum or Kayseri would dominate in thickness requirements.
- Traffic volume influenced thickness less than expected, with increases averaging only 5–8%. This limited impact is due to small slab sizes and the localized nature of wheel loading in BCOA, where fatigue is governed more by stress ratios than total ESALs.
- Subgrade effect varied by slab size and small slabs were less sensitive to subgrade stiffness (k-value) changes. On the other hand, large slabs showed up to 15% reduction in thickness when moving from poor to good subgrade support, due to higher deflection sensitivity.
- Wheel wander effects design stress on small and large slabs, as it is only modeled for slabs larger than 4.5 ft (1.5m). This leads to increased effective fatigue life for large slabs and can sometimes result in similar or lower thickness than smaller slabs.
- Joint spacing behavior was influenced by fiber. Without fiber, smaller slabs consistently resulted in thinner overlays. With fiber, the thickness difference between small and large slabs diminished, allowing for potentially wider joint

spacing with fiber reinforcement. However, this observation should be experimentally validated, particularly for its influence on LTE.

- The condition of the existing asphalt (HMA) had a limited effect. Comparing “adequate” vs. “marginal” pavement support resulted in no more than 5% change in thickness. This is due to the dominance of the concrete overlay’s stiffness and the indirect way BCOA-ME adjusts for asphalt degradation.
- A user-friendly digital tool was developed, allowing engineers to select design parameters and obtain recommended thicknesses for each city in Türkiye. This tool serves as a valuable aid for early-stage project evaluation and can be accessible via QR code and link.

Given the dominance of asphalt pavements in Türkiye's national highway network and the significant increase in freight and passenger transport demand, BCOA stand out as one of the most practical and promising strategies for pavement rehabilitation. Since most of the existing road infrastructure is composed of flexible pavements, the use of relatively thin concrete overlays provides an efficient way to significantly extend service life without the need for full-depth reconstruction. BCOA offer a cost-effective, durable, and structurally sound solution, especially under increasing traffic volumes and environmental loading. Therefore, adopting BCOA as a alternative rehabilitation approach holds strong potential for improving the performance and sustainability of Türkiye’s Road infrastructure.

6.2 Recommendations and Future Works

The ultimate goal of this parametric study is to support the development of a locally adapted, performance-based M-E design methodology for BCOA adapted to Türkiye’s unique infrastructure, local materials, and climate conditions. This study represents the first phase of that goal, utilizing the existing BCOA-ME framework developed by the University of Pittsburgh to produce preliminary thickness design charts. These initial outputs provide valuable guidance to engineers, contractors, and public agencies during early decision-making, feasibility analysis, and bidding processes—especially in cases where only default input parameters are available.

Future efforts should focus on the experimental validation of fiber-reinforced overlays, particularly regarding their structural effects on joint spacing and load transfer efficiency. As this study highlighted, fiber content plays a significant role in overlay thickness, but further laboratory and field studies are essential to better understand and calibrate these effects. These findings will be effective in strengthening the theoretical foundation of future design tools. Ultimately, the aim is to develop a fully calibrated M-E design methodology for Türkiye by incorporating national climate data, regional material properties, and long-term performance monitoring. This localized framework will allow for more reliable, cost-effective, and sustainable overlay solutions across a wide range of pavement rehabilitation projects in Türkiye.

REFERENCES

[1] Smith K. D., Yu H. T., & Peshkin D. G., *Portland Cement Concrete Overlays State of Technology Synthesis*. Federal Highway Administration. Tech. Report: FHWA-IF-02-045. 2002.

[2] Dufalla N., Li Z. & Vandenbossche, J. M. *Bonded Concrete Overlay of Asphalt Pavements Mechanistic-Empirical Design Guide (BCOA-ME): User's Guide*. University of Pittsburgh. 2021.

[3] Desantis, J.W. Modeling the Development of Joint Faulting for Bonded Concrete Overlays of Asphalt Pavements (BCOA), doctoral dissertation, University of Pittsburgh. 2020.

[4] Karayolları Genel Müdürlüğü (KGM). *Yol Ağı Bilgileri*. Ankara, Turkiye. 2025.

[5] Karayolları Genel Müdürlüğü (KGM). *2023 Faaliyet Raporu*. Ankara, Turkiye; Strateji Geliştirme Dairesi Başkanlığı. 2023.

[6] Karayolları Genel Müdürlüğü (KGM). Karayolu Ulasim Istatistikleri. Ankara, Turkiye. 2023.

[7] Sengun, E., Yaman, I.O., & Ceylan, H. An Overview on Rigid Pavement Specifications in Developed Countries. *Cement and Concrete World*, pp. 58–67, 2016. Available: https://www.researchgate.net/publication/324537352

[8] İstanbul Büyükşehir Belediyesi. Metrobüs Hattı 'Beyaz Yol' Konforuna Kavuştu. Retrieved from: https://uym.ibb.gov.tr/kurumsal/haberler-ve-duyurular/metrobüs-hattı-'beyaz-yol'konforuna-kavuştu. 2023.

[9] Komut, M., Ünal, E., & Altiok, Ş. Karayolları Genel Müdürlüğü ağındaki beton deneme yolların performans değerlendirmesi. 2019.

[10] Taher, S., Alyousify, S., & Hassan, H. Comparative Study of Using Flexible and Rigid Pavements for Roads: A Review Study. *The Journal of the University of Duhok*, *23*, 222–234.2020.

[11] McGhee, K. H. Portland Cement Concrete Resurfacing – A Synthesis of Highway Practice. 1994.

[12] Harrington, D.S., *Guide to concrete overlays for resurfacing & rehabilitating existing pavements*-Iowa DOT Seminar. 2008.

[13] Hanson, T. *Guide to Concrete Overlays*, 3rd ed. 2014.

[14] Fick, G., Gross, J., Snyder, M. B., Harrington, D., Roesler, J., & Cackler T., Guide to Concrete Overlays, 4th ed. 2021.

[15] Vandenbossche, J.M., & Sachs, S. *Guidelines for Bonded Concrete Overlays of Asphalt: Beginning with Project Selection and Ending with Construction*. 2013.

[16] Fick, G., & Harrington, D. Bonded Concrete Overlays Over Asphalt (BCOA). 2015.

[17] Torres, H.N., Roesler, J., Rasmussen, R.O. & Harrington, D. *Guide to the design of concrete overlays using existing methodologies*. 2012.

[18] Vandenbossche, J.M., & Barman, M. Bonded Whitetopping Overlay Design Considerations for Prevention of Reflection Cracking, Joint Sealing, and the Use of Dowel Bars. *Transportation Research Record*, pp. 3–11. 2010.

[19] Huang, Y.H., *Pavement Analysis and Design* (2nd ed.), USA: Prentice Hall. 2004.

[20] Arhin, S.A., Noel, E.C., Wright, D., Khan, W., & Hong, V. Exploring the use of the saw and seal method for mitigation of reflective cracking in composite pavements. *In WIT Transactions on the Built Environment*, pp. 527–537.2012.

[21] Öztaş, G., Sütaş, İ., & Ağar, E. Beton asfalt kaplama ile beton yol karşılaştırması. *İMO İzmir Şubesi*, *119*. 2004.

[22] Roesler, J., Bordelon, A., Ioannides, A., Beyer, M., & Wang, D. *Design and Concrete Material Requirements for Ultra-Thin Whitetopping*. 2008.

[23] Barman, M., Vandenbossche, J.M., & Li, Z. Influence of Interface Bond on the

Performance of Bonded Concrete Overlays on Asphalt Pavements. *Journal of Transportation Engineering, Part B: Pavements*, *143*. 2017.

[24] Mateos, A., Millan, M.A., Harvey, J.T., Paniagua, F., & Wu, R. Mechanisms of Asphalt Cracking and Concrete-Asphalt Debonding in Concrete Overlay on Asphalt Pavements. *Construction and Building Materials*, 124086. 2021.

[25] Isla, F., Luccioni, B., Ruano, G., Torrijos, M.C., Morea, F., Giaccio, G., & Zerbino, R. Mechanical Response of Fiber Reinforced Concrete Overlays over Asphalt Concrete Substrate: Experimental Results and Numerical Simulation. *Construction and Building Materials*, *93*, 1022–1033. 2015.

[26] Roesler, J., Bordelon, A., Brand, A. S., & Amirkhanian, A. Fiber-Reinforced Concrete for Pavement Overlays: Technical Overview Final Report. Iowa State University, Part of Intrans Project 15-532, TPF-5(313). 2019.

[27] Bordelon, A., & Roesler, J. Design with fiber reinforcement for thin concrete overlays bonded to asphalt. *Journal of Transportation Engineering*, *138*, 430–435. 2012.

[28] Markovic, I., *High-Performance Hybrid-Fibre Concrete - Development and Utilisation*, DUP Science, Delft. 2006.

[29] Blazy, J., & Blazy, R., Polypropylene fiber reinforced concrete and its application in creating architectural forms of public spaces. *Case Studies in Construction Materials, 14*. 2021.

[30] Öztürk, H.I., Tan, E.B., Şengün, E., & Yaman, İ.Ö. Farklı trafik, zemin, malzeme ve iklim koşulları için mekanistik-ampirik (M-E) yöntemle tasarlanan derzli donatısız rijit üstyapı sistemlerinin karşılaştırılması. *Gazi Üniversitesi Mühendislik-Mimarlık Fakültesi Dergisi*, *34(2)*, 771–784. 2019.

[31] Öztürk, M.Z., Çetinkaya, G., & Aydın, S. Köppen-Geiger İklim Sınıflandırmasına Göre Türkiye'nin İklim Tipleri. *Journal of Geography*, *35*, 17–27. 2017.

[32] American Association of State Highway and Transportation Officials

(AASHTO). *Guide for the Design of Pavement Structures*, Washington, DC, 1993.

[33] Li Z., Dufalla, N., Mu, F., & Vandenbossche, J. *Bonded Concrete Overlay of Asphalt Pavements Mechanistic-Empirical Design Guide (BCOA-ME) Theory Manual.* Pittsburgh, Pennsylvania. 2021.

[34] Mu, F., & Vandenbossche, J. Establishing effective linear temperature gradients for ultrathin bonded concrete overlays on asphalt pavements. *Transportation Research Record*, 24–31. 2012.

[35] Larson, G., & Dempsey, B.J. *Enhanced Integrated Climatic Model Version 2.0.* 1997.

[36] DeSantis, J.W., Vandenbossche, J.M., & Sachs, S.G. Artificial Neural Networks for Predicting the Response of Unbonded Concrete Overlays in a Faulting Prediction Model. *Transportation Research Record*, *2673*, 762–769. 2019.

[37] Kaşak, S., & Komut, M. *Karayolları Beton Yol Üstyapılar Projelendirme Rehberi*. Ankara, Turkiye; Araştırma ve Geliştirme Dairesi Başkanlığı. 2019.

[38] American Concrete Pavement Association (ACPA). *Database of State DOT Concrete Pavement Practices*. Skokie, IL: American Concrete Pavement Association. 2006.

[39] Paul, S.C., Van Zijl, G.P.A.G., & Šavija, B. Effect of fibers on durability of concrete: A practical review. Materials, *13*,1–26. 2020.

[40] King, D., & Roesler, J. Structural Performance of Ultra-Thin Whitetopping on Illinois Roadways and Parking Lots: Findings of ICT-R27-61 Mechanistic-Empirical Design Implementation and Monitoring for Rigid Pavements. 2014.

[41] Altoubat, S. A., Roesler, J. R., Lange, D. A., & Rieder, K. A. Simplified Method for Concrete Pavement Design with Discrete Structural Fibers. *Construction and Building Materials*, *22*, 384–393. 2008.

[42] Covarrubias, J.P., & Roesler, J. Design of Concrete Slabs with Optimized

Geometry. 11th International Symposium on Concrete Roads, Spain, pp. 13–15, 2010.

[43] Riley, R. C. Incorporation of Probabilistic Concepts into Fatigue Analysis of Ultra-Thin Whitetopping as Developed for American Concrete Pavement Association. 2005.

[44] A. Jihad, H. Rami, J. Aghajan, S. Lecturer, & P. Candidate. Flexural and Flexural Toughness of Fiber Reinforced Concrete-American Standard Specifications Review. *Global Research and Development Journal for Engineering*, *4*, 2019.

[45] Kaplanca D., Şengün E. Designing Fiber-Reinforced Concrete Overlays Adapted To Cold Climate Regions in Türkiye. 3rd International Karatekin Science and Technology Conference, p. 6, 2024.